Industrial Scale Production of the R21c/Matrix-M Malaria Vaccine for Sub-Saharan Africa

A Technical Report submitted to the Department of Chemical Engineering

Presented to the Faculty of the School of Engineering and Applied Science
University of Virginia • Charlottesville, Virginia

In Partial Fulfillment of the Requirements for the Degree
Bachelor of Science, School of Engineering

Anupama Jayaraman

Spring, 2023

Technical Project Team Members
Sierra Giles
Ian Lucas
Jacob Wilkins
William Wonsik

On my honor as a University Student, I have neither given nor received unauthorized aid on this assignment as defined by the Honor Guidelines for Thesis-Related Assignments

Advisor

Eric Anderson, Department of Chemical Engineering

Table of Contents

I. Executive Summary

While still undergoing clinical testing, the R21c/Matrix-M vaccine is the most effective alternative to the existing malaria vaccine on the market. As a result, the production of the R21c vaccine, to serve infants and children in sub-Saharan Africa (SSA), will prove important to lessen the burden of malaria on individuals and countries.

The described manufacturing process, to meet the estimated demand in SSA, begins with fermentation in shake flasks, small bioreactors, and a production-size bioreactor specially designed for plant operation. In these steps, *Pichia pastoris* yeast cells, genetically modified to express the R21c fusion protein antigen under methanol exposure due to the control by the AOX1 promoter, are grown. The harvested cells are fed into the downstream process, which begins with centrifugation and high pressure homogenization steps to lyse the yeast and release and isolate the R21c protein, which spontaneously assembles into its vaccine-like particle (VLP) form upon lysis. Depth-filtration aids in removing remaining cell debris to improve purity and prevent equipment fouling. Subsequently, two chromatography steps are formed. First, Capto Core 700, a modified form of size exclusion chromatography, removes small impurities that persist in solution. The remaining large impurities, including AOX1, are removed through C-tag affinity chromatography, which uses a resin that binds to a C-terminus tag on the R21c proteins to allow for better purification efficiency. After the chromatography steps, a diafiltration step will exchange the buffer solvent with water for injection (WFI). After resuspending the protein at the desired concentration, sterile filtration removes any viruses, microorganisms, and endotoxins that are present in the solution. Single-dose vaccine vials are then filled with the R21c solutions and undergo lyophilization. Production of Matrix-M, the adjacent that facilitates the vaccines high efficacy, is outside of the scope of the presented plant design and will be purchased from

Novavax. Due to differences in storage conditions, the R21c VLPs will be mixed with Matrix-M just prior to injection. Operating with 13 batches per year, the proposed plant will produce 3.3 kg of R21c, enough for 21.8 million vaccines, and will operate for 266 days each year.

To determine financial feasibility, various scenarios were considered over 20 years of operation. Under conservative selling estimates, and pricing each dose at a ceiling of $3, annual revenue is expected to be $816 million. With an initial capital cost investment of $48 million, plus an annual operating cost of $193 million, the predicted 20-year net present value of the plant reaches $3.4 billion and the return on investment is 7100%. In best and worst case scenario estimates, the 20-year return on investments range from 3381% to 7480%. Thus, due to the high return on investment, pursuit of the proposed R21c vaccine manufacturing plant is highly recommended.

II. Body of Report

A. Introduction

In 2019 alone, there were 228 million reported cases and 405 thousand deaths as a result of malaria, which remains one of the leading causes of morbidity and mortality in the developing world. Currently, there are five *Plasmodium* parasites that are known to cause malaria in different parts of the world. Of these five, *Plasmodium falciparum*, the parasite implicated in severe malaria cases and over 90% of world mortality due to malaria, is most common in sub-Saharan Africa (SSA) (Figure A1). There, malaria is endemic and children younger than five-years old are the most at risk (Price et al., 2020; Zekar & Sharman, 2022) at contracting the disease as they have not yet developed natural immunity to the infection (Cowman et al., 2016).

Figure A1

Frequency of P. falciparum Malaria Cases in 2017
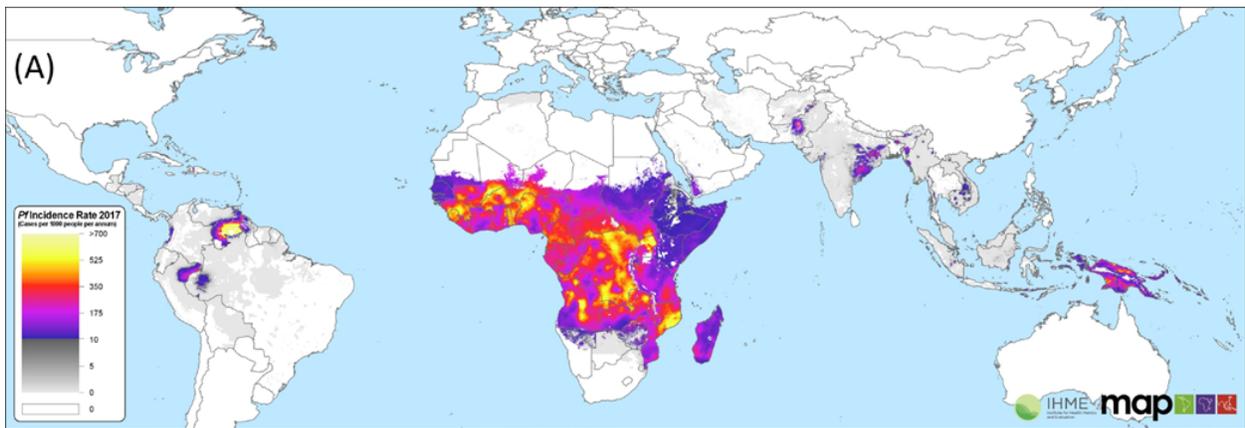
Note. This figure demonstrates that while there are cases elsewhere, the primary regions in the world with a high incidence rate of *P. falciparum* malaria are Sub-Saharan African countries. Adapted from (Price et al., 2020)

Malaria infections are spread between people via the *Anopheles* mosquito vector, which allows the parasite to enter the blood, and subsequently infect hepatocytes and erythrocytes, eventually leading to red blood cell lysis (Talapko et al., 2019). The infection results in high fevers and non-specific symptoms, including nausea and muscle pain. Extreme malaria cases may result in severe anemia, comas, and respiratory distress, in addition to death. Although artemisinin-based drug therapies can treat symptoms and completely eradicate the infection from the blood, due to drug resistance, *P. falciparum* can persist in the blood asymptomatically, causing recrudescence, a repeated malaria attack in the infected host, and serving as a source of further parasite spread (Cowman et al., 2016). As a result, there is a need for an effective malaria vaccine to limit the burden of *P. falciparum* malaria on individuals.

1. Previous Technology

Currently, the RTS,S/AS01 anti-sporozoite vaccine, developed by GlaxoSmithKline, is the only approved vaccine for malaria that has been recommended for widespread use by the World Health Organization (WHO) in endemic regions (D'Souza & Nderitu, 2021). The vaccine is a virus-like particle (VLP) that presents the circumsporozoite protein (CSP), a protein on *P. falciparum* that is critical for infecting host cells, by linking it to the hepatitis B surface antigen (HBsAg). The saponin-based AS01 adjuvant is mixed with the VLP to enhance the effectiveness of the vaccine (Nadeem et al., 2022). Clinical trial data demonstrate that the vaccine significantly reduces hospital admissions associated with malaria (RTS,S Clinical Trials Partnership, 2015). Unfortunately, at 48 months following the initial three-dose vaccination, the vaccine had only a 36% efficacy in children (5-17 months at receipt of vaccine) and a 26% efficacy in infants (6-12 weeks at receipt of vaccine). Additionally, RTS,S/AS01 efficacy gradually declined over time, with a possible negative efficacy in regions with higher-than-average exposure to *P. falciparum*

(Olotu et al., 2016). Other malaria vaccines, like PfSPZ, a radiation attenuated vaccine, also lack efficacy in preventing infections (Oneko et al., 2021) and do not meet the WHO-specified 75% efficacy goal for malaria vaccines. However, scientists at Oxford University recently developed the first vaccine to meet the goal: the R21/M-Matrix vaccine.

2. Drug Product: R21c/Matrix-M

R21/M-Matrix is a pre-erythrocytic malaria vaccine that improves the RTS,S/A01 vaccine design. One of the primary structural issues with RTS,S/A01 is the low proportion of CSP to HBsAg, which shifts the immune response away from CSP and towards HBsAg, effectively providing no protection against malaria. By modifying the vaccine synthesis method to increase the proportion of accessible CSP (Figure A2-1) and minimize external access to the HBsAg, Oxford scientists were able to develop a more immunogenic VLP. This particle is able to activate both cellular and humoral responses unlike RTS,S/A01, which primarily functions through a humoral response (K. A. Collins et al., 2017). Recent clinical trial data shows that 24 months after initial vaccination, the R21 vaccine has an 80% efficacy against malaria in children (5-17 months at receipt of vaccine) when mixed with Matrix-M (Datoo et al., 2022), a saponin adjuvant developed by Novavax that enhances the immune response (Reimer et al., 2012). In addition to the higher efficacy, R21/Matrix-M is superior to RTS,S/A01 as it is easier to develop and cheaper (Mandavilli & Cheng, 2022). Currently, the vaccine is manufactured by the Serum Institute of India, facilitating a 30 times larger production scale than RTS,S (Ledford, 2022). Although the vaccine is still undergoing clinical trials to confirm its efficacy, R21/M-Matrix is a promising candidate for widespread use in SSA.

In this project, we will be adding a C-tag to our protein and producing R21c/Matrix-M (Figure A2-1) instead of R21/Matrix-M. This E-P-E-A C-terminus tag can significantly increase

the purity of our VLP under cGMP conditions. Specifically, the C-tag is conducive to efficient separation via affinity chromatography (Mukhopadhyay et al., 2022). In addition, R21c demonstrates a good safety profile with comparable immunogenicity to R21 (K. Collins et al., 2021). The Clinical Biomanufacturing Facility (CBF, Oxford) produced R21c vaccines for Phase I clinical trials in healthy UK and Burkina Faso adults and yielded positive results, further implying the safety and efficacy of the modified vaccine in humans (Datoo et al., 2021).

Figure A2-1

Comparison of fusion proteins used in malaria vaccines
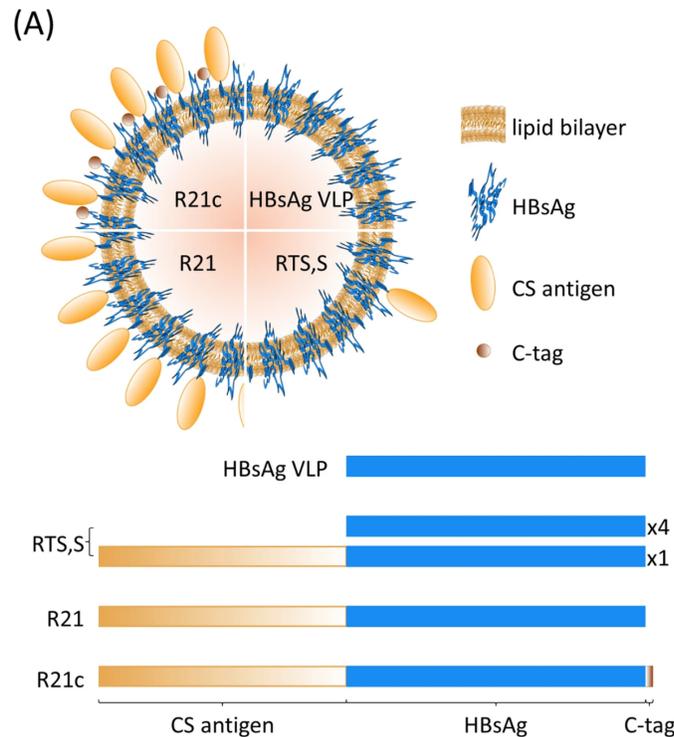
Adapted from (K. Collins et al., 2021)

Currently, the R21/Matrix-M vaccine is undergoing Phase III clinical trials in Burkina Faso, Kenya, Malia, and Tanzania and published results are expected by the end of 2023. Preliminary results support Phase II results regarding the vaccine's high efficacy. As of April

24th, 2023, Ghana and Nigeria have approved the vaccine for use in children aged five to 36 months (Joi, 2023; Rachini, 2023).

3. Product Specification

The R21c particle is 22 nm in diameter and is composed of a lipid bilayer with embedded CSP-HBsAg fusion protein (Figure A2-1), which is ~45.3 kDa in mass. These particles express a CSP portion of the fusion protein at high densities on their surfaces, while the HBsAg portion forms the core of the particle and is blocked from exposure to the immune system by the CSP. The particles have a density of 1.2 g/mL, mass of 4029 kDa, and theoretical pI of 7.85. The chemical formula of the fusion protein that makes up the VLP is $C_{2019}H_{3071}N_{545}O_{594}S_{27}$ (K. A. Collins et al., 2017; *ExPASy - ProtParam Tool*, n.d.). In clinical trials, the most effective vaccine contained 5 µg R21c and 50 µg Matrix-M adjuvant, a 1:10 ratio of R21c to Matrix-M (Datoo et al., 2022). As a result, we will formulate our vaccine according to these specifications, with an aim to meet a >99% purity standard.

4. Scale of Project & Location

There are approximately 200 million children under age five in Sub-Saharan Africa and 40 million children are born each year (*Sub-Saharan Africa*, n.d.). Our goal is to generate supply to vaccinate 70%, WHO's COVID-19 vaccination goal, of new births each year, the most susceptible population. In an attempt to supply vaccines to other susceptible children, we will produce enough vaccines for 20% of all children under five years old. Full vaccination requires four doses, consisting of three primary doses and one booster. As a result, 272 million vaccines are necessary to meet our target. Each vaccine dose will be sold for $3.00, the ceiling price for COVID-19 vaccines distributed by Gavi and the Gates Foundation to low-income countries

(Gavi Staff, 2020). This price yields an expected revenue of $816 million annually (Table A4-1). Given that there are 5 µg R21c in each vaccine, we must produce 1.36 kg of purified R21c annually. We will license the corresponding 13.6 kg of Matrix-M from Novavax to complete our vaccine (Datoo et al., 2022).

Table A4-1

Calculation of Vaccine Production Goal & Expected Revenue

Population Type	Population Size	Vaccine Coverage	Total People to Vaccinate	Total # Vaccines
SSA <5 yrs	200,000,000	20%/year	40,000,000/year	160,000,000 /year
SSA birth rate	40,000,000/year	70%	28,000,000/year	112,000,000 /year
			Total vaccines to produce:	272,000,000 /year
			Total Expected Revenue:	$816,000,000 /year

We aim to produce the R21c/Matrix-M vaccines in South Africa to be close to the target population. The facility will be co-located with Biovac's manufacturing plant in Cape Town, South Africa, which produces COVID-19 vaccines in partnership with Pfizer and BioNTech (*Pfizer and BioNTech Announce Collaboration With Biovac to Manufacture and Distribute COVID-19 Vaccine Doses Within Africa*, 2021). It is beneficial to work in conjunction with an existing facility due to the relatively small size of the designed production plant. This allows for reduced capital costs, an existing water-for-injection (WFI) system in place, and backup power if

necessary. Additionally, with proposed batch scheduling, there will be off time where no R21c production occurs. During this time, Biovac may rent facility resources to meet their production demand. Building the plant in sub-Saharan Africa will reduce the time and distance required to vaccinate the public thus decreasing distribution costs. Furthermore, by putting the vaccine production facility in Africa the plant will promote further growth in the pharmaceutical sector in a region otherwise underdeveloped in manufacturing. As a result of placing our plant in South Africa, the produced vaccines will be regulated by the South African Health Products Regulatory Authority (SAHPRA).

B. Discussion of Proposed Manufacturing Train

In anticipation of vaccine approval, this project aims to develop a safe and cost-effective process to manufacture R21c/Matrix-M for use in preventing malaria infections in Sub-Saharan Africa. The process will involve upstream, downstream, and formulation & fill-finish stages (Figure B1) and describe the industrial scale production of single-dose vaccines. Figures D1-1, D1-2, and D1-3 depict the process flow diagram for upstream, downstream, and formulation & fill-finish, respectively.

Figure B1

Block Flow Diagram for Proposed R21c Manufacturing Process
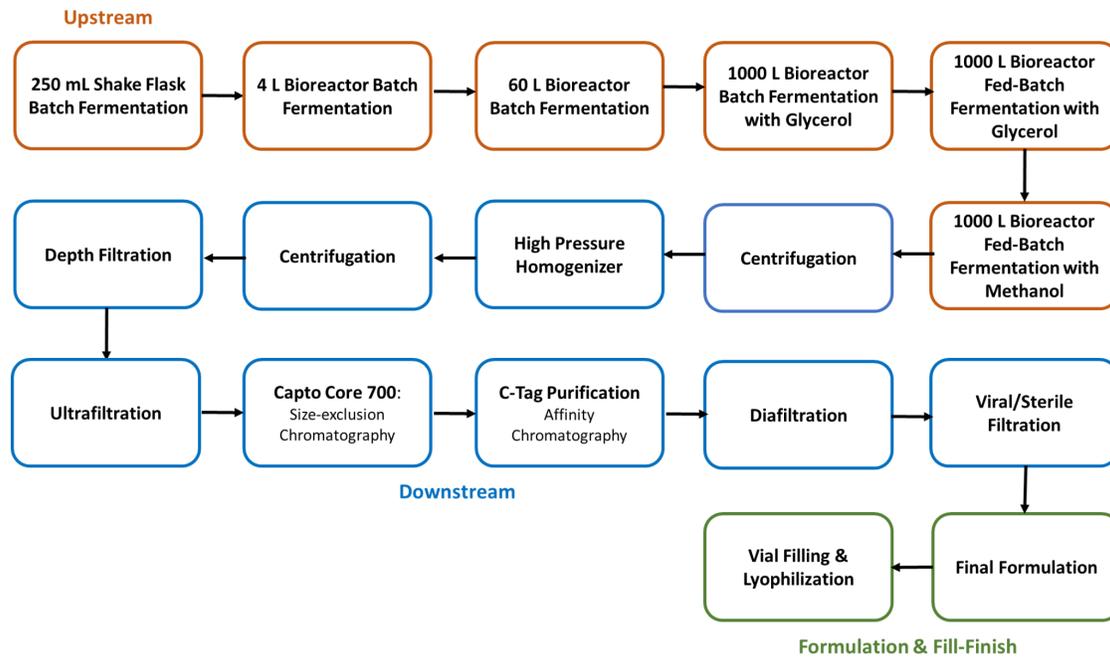
1. Upstream

1.1 Microbe: *P. pastoris*

For R21c production, we will be using the yeast *Pichia pastoris*. This yeast is key to the production process as it is able to grow to, and express proteins at, high enough densities to facilitate the spontaneous formation of the R21c particle after cell lysis (K. A. Collins, 2014). The specific strain of *P. pastoris* we are using in our production process will be acquired from the Clinical Bio-Manufacturing Facility (CBF) at Oxford, which produced the R21c/Matrix-M vaccines for Phase I of clinical trials (Datoo et al., 2021). We will be acquiring this strain of cells as frozen vials (concentration of 0.25 g cells/mL media) via a partnership with CBF.

This *P. pastoris* strain has the phenotype of GS115 Mut⁺ His⁻, which allows the yeast cells to produce target proteins only under exposure to methanol (MeOH). In the specific strain we will be using, the gene encoding R21c has been inserted into the AOX1 gene (Figure B1-1), such that R21c is tightly regulated by an MeOH inducible promoter. As a result, growth and recombinant protein production with *P. pastoris* typically occurs in three phases of growth: glycerol batch, glycerol fed-batch, and MeOH fed-batch. The glycerol batch phase serves to increase biomass concentration, the glycerol fed-batch phase serves to ease the yeast into the transition to MeOH from glycerol feed, and the final MeOH fed-batch phase is to produce the target protein. This procedure enables us to grow the yeast cells to a high density, under exposure to glycerol, before inducing R21c fusion protein production. As a result, the method effectively eliminates the negative accumulation effect of the fusion protein concentration on biomass production, allowing for much higher protein yield than with typical joint cell growth and protein production (K. A. Collins, 2014; Cregg et al., 2000; Stratton et al., 1998).

Figure B1-1

P. pastoris Recombinant Gene Diagram
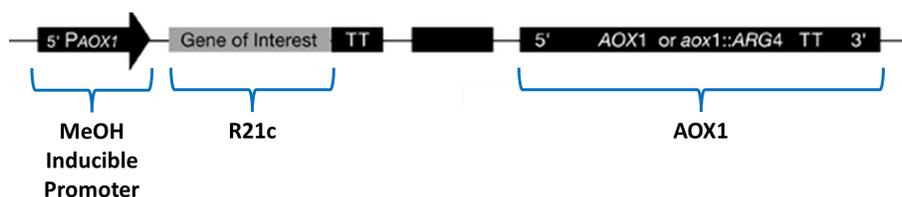
Adapted from (Li et al., 2007)

Optimal growth parameters for *P. pastoris* are 30℃, > 20% dissolved oxygen (DO), and 5.5 pH. All bioreactors for yeast fermentation in our process will run under these conditions (Invitrogen, 2002).

1.2 Seed Train

To grow cells to the desired density in our production bioreactor, we need to first incrementally increase the quantity of cells through a seed train with glycerol batches. This procedure will consist of three increasing bioreactor working volumes: 250 mL (R101), 2.5 L (R102), and 50 L (R103). These volumes adhere to the *P. pastoris* fermentation guideline of inoculating each fermenter with 5-10% initial fermentation volume from the cell culture produced in the previous bioreactor step (Invitrogen, 2002).

For modeling these glycerol batch-growth bioreactors, we require kinetic parameters that describe the system. In order to obtain some of the necessary yield coefficients, and to satisfy material balances, we balanced the chemical equation for cell growth and respiration under glycerol (Equation B1-1) and methanol (Equation B1-2). Here, we simplify the balance by removing all nitrogen and sulfur atoms from the molecular representation of *P. pastoris* (Jordà et al., 2012) and R21c. We also used biomass and product yield coefficients from literature to solve for the coefficients. Table H1 and H2 (Appendix) list all of the literature and chemical balance-derived kinetic constants, respectively, that will be used for modeling upstream. For the purpose of modeling upstream and satisfying material balances, we will use the yield constants derived from Equations B1-1 and B1-2.

$$\text{Equation B1-1. } C_3H_8O_3 + 0.6\,O_2 \rightarrow 2.6\,CH_{1.761}O_{0.636} + 1.7\,H_2O + 0.4\,CO_2$$

$$\text{Equation B1-2.}$$

$$CH_4O + 0.8\,O_2 \rightarrow 0.6\,CH_{1.761}O_{0.636} + 1.5\,H_2O + 0.4\,CO_2 + 4*10^{-7}C_{2019}H_{3071}O_{594}$$
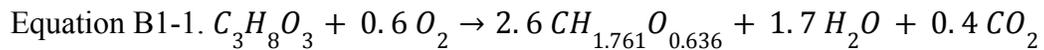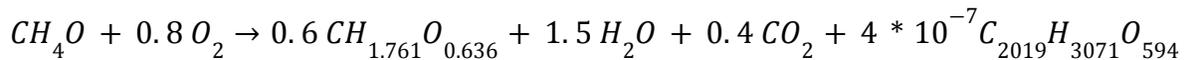
For modeling the reactors, we assume Type 1 growth and Monod kinetics. This allows us to represent the system with Equations B1-(3-11). Here, X^t is the total biomass of *P. pastoris* (g), μ is the specific growth rate (h^{-1}), S^t is the total substrate (g), S_{in} is the concentration of the substrate flowing into the reactor (g/L), F is the flowrate of the substrate (L/h), $Y_{X/S}$ is the yield coefficient of biomass from substrate (g/g), P^t is the total amount of R21c (g), and $Y_{P/S}$ is the yield coefficient of product from substrate (g/g) (Prpich, 2021b). O_2^t, CO_2^t, and N_2^t are the total oxygen, carbon dioxide, and nitrogen in the system, respectively. H_2O^t is the total amount of water produced through cellular processes and $H_2O^{t, vap}$ is the amount of that water that exits the reactor as a vapor. $H_2O^{t, vap}$ is computed with the function $m_{H2O,vap}$ at 1 atm, such that the mole fraction of H_2O among the other outlet gasses (O_2, N_2, CO_2) is equivalent to 0.0419 atm, the saturation pressure of H_2O at 30°C, (The Engineering ToolBox, 2004). Finally, V^t is the volume of fluid in the bioreactor at a given time. This value is influenced by the amount of substrate added to the reactor, as well as the non-vaporized water that is produced by the reaction. For model simplification, we assume that there is no O_2 lost to dissolution in the water or broth. Using this system of ordinary differential equations, we modeled the concentration of biomass, substrate, and product in each step of the seed train (Figure B1-2).

$$\text{Equation B1-3. } \frac{dX^t}{dt} = \mu X^t$$

$$\text{Equation B1-4. } \frac{dS^t}{dt} = FS_{in} - \frac{1}{Y_{X/S}}\frac{dX^t}{dt}$$

$$\text{Equation B1-5. } \frac{dP^t}{dt} = Y_{P/S}\frac{dS^t}{dt}$$

$$\text{Equation B1-6. } \frac{dO_2^t}{dt} = m_{O_2} - \frac{1}{Y_{X/O2}}\frac{dX^t}{dt}$$

$$\text{Equation B1-7.} \quad \frac{dCO_2^t}{dt} = RQ * \frac{1}{Y_{X/O2}} \frac{dX^t}{dt}$$

$$\text{Equation B1-8.} \quad \frac{dN_2^t}{dt} = m_{N_2}$$

$$\text{Equation B1-9.} \quad \frac{dH_2O^t}{dt} = Y_{H2O/O2} * \frac{1}{Y_{X/O2}} \frac{dX^t}{dt}$$

$$\text{Equation B1-10.} \quad \frac{dH_2O^{t,\,vap}}{dt} = m_{H_2O,\,vap}(\frac{dO_2^t}{dt}, \frac{dCO_2^t}{dt}, \frac{dN_2^t}{dt})$$

$$\text{Equation B1-11.} \quad \frac{dV^t}{dt} = F + (\frac{dH_2O^t}{dt} - \frac{dH_2O^{t,\,vap}}{dt})/\rho$$

According to our model, R101 starts with 250 mL of MGY Media (Table H3), with 10 g/L glycerol, and will be inoculated with a thawed, 1 mL vial of frozen cells. Air will be fed into the vessel at a rate of 0.0015 m^3/h dry air (21% O_2, 79% N_2). Assuming no lag phase in the growth of the cells, we reach steady state concentrations at around 9.5 hours. To maximize yield in our process, we want to minimize the stationary phase and prevent cell death and excess water from leaving with air flowing in. Thus, we will end the R101 batch after 9.5 hours of operation. For this unit, we will use the 1 L Corning® Erlenmeyer cell culture flasks from SigmaAldrich (SigmaAldrich, n.d.). These flasks will operate with standard sterilization protocols in place. The protocols involve autoclaving the culture flasks, followed by washing them with detergent (*Cleaning Laboratory Glassware*, n.d.).

Figure B1-2

Concentration Curves for Seed Train
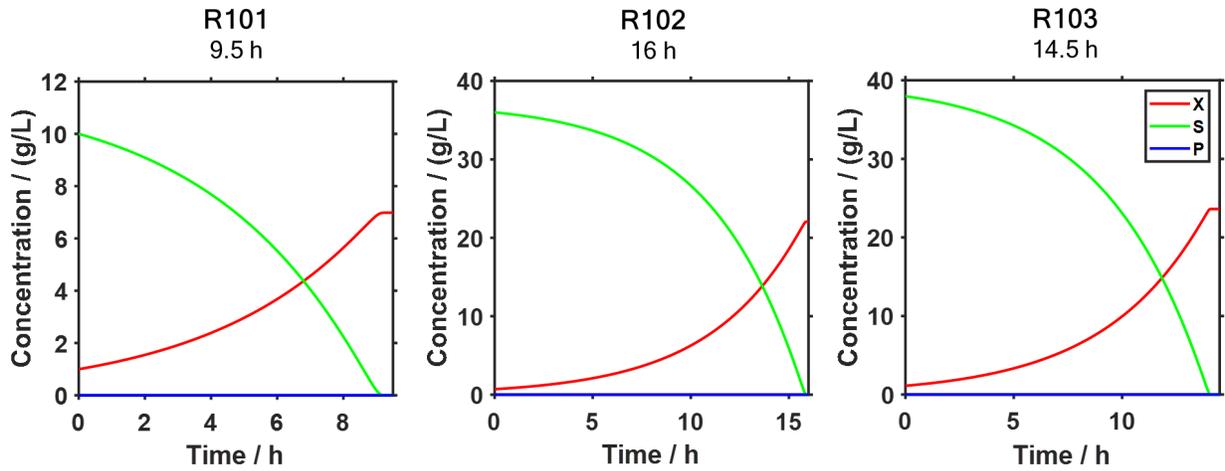
The final contents of R101 will then be poured into R102, in which we will add Basal

Salts media (Tables H4 and H5), at 40 g/L glycerol, until the bioreactor has 2.5 L of volume. Air

will be fed into the bioreactor at a rate of 0.015 m³/h dry air and we will run R102 for

approximately 16 hours until the system reaches steady state. Subsequently, we will pump the

contents of R102 in R103, add enough Basal Salts media to reach a volume of 50 L, and run the

reactor for 14.5 hours, while flowing in dry air at 0.30 m³/h. We will be using the Allegro™ XRS

25 Bioreactor System, which can handle 2-25 L of working volume (Pall Corporation, n.d.-b),

and the Allegro ™ STR Single-use Stirred Tank Bioreactor, which can handle ~50 L of working

volume (Pall Corporation, n.d.-a), for R102 and R103, respectively. Both of these bioreactors

will operate with single-use, plastic fermentation bags.

1.3 Production Bioreactor

The contents of R103 will be pumped into our production bioreactor, R104. This

production bioreactor will contain all three phases of growth for recombinant protein production.

As a result, this bioreactor will be designed to accommodate an initial glycerol batch phase, followed by two fed-batch stages. To prevent too much change in operating conditions between each phase, we will be flowing in dry air at a constant rate of 27 m³/h and temperature of 20°C throughout the process.

After R103 has been pumped into R104, Basal Salts and PTM1 media are added until the fermentation volume reaches 1000 L. This initial phase of glycerol batch growth (phase 1) occurs for approximately 14 hours. Subsequently, 30°C glycerol feed (Table H6) is added to the bioreactor at a rate of 18.15 L/h, for the following four hours (Invitrogen, 2002). To model the fed-batch growth kinetics, we continue to use Equations B1-(3-11) (Figure B1-3). Model results demonstrate that at the end of the glycerol fed-batch stage (phase 2), the total fermentation volume is ~1085 L. For modeling the subsequent 70 hour MeOH fed-batch phase (phase 3), during which time we see the production of R21c, we substituted the relevant chemical balance-derived MeOH kinetic parameters (Table H2) into the equations. During this phase, 30°C MeOH feed (Table H7) is added to R104 at a rate of 3.6 L/h for the first four hours, 7.3 L/h for the next two hours, and 10.9 L/h for the rest of the process. This stepped addition of MeOH helps the yeast gradually adjust to the addition of MeOH and maintain productivity (Invitrogen, 2002). Throughout both of the fed-batch phases, the substrate concentration of glycerol and MeOH are close to 0 as they are being consumed almost instantaneously by the yeast in solution. At the end of this process, the total fermentation volume will be ~2230 L and R104 will have been running for 88 hours. We estimate that we will produce 256 g of R21c within the yeast cells at the end of this fermentation step. The overall material balances across all upstream streams are provided in Table D2-1.

Figure B1-3

Concentration Plot for R104
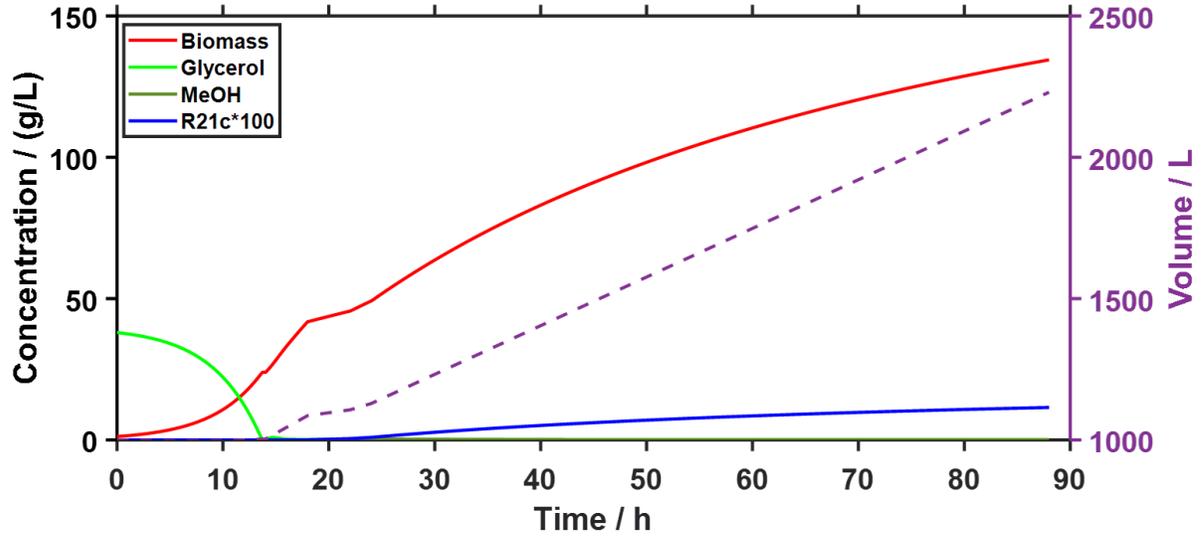
1.3.1 Reactor Design

To design R104, we need to understand oxygen transfer throughout the bioreactor. We first estimated the oxygen utilization rate (OUR; g/L/h) of *P. pastoris* across the bioreactor run using Equation B1-12, where $Y_{X/O2}$ (g/g) is yield coefficient for biomass from O_2. Figure B1-4 depicts the OUR for the different $Y_{X/O2}$ values we have. For conservative estimates with bioreactor design, we will use the OUR determined by literature values. The peak OUR in R104 is at approximately 25 hours, within the MeOH fed-batch phase of growth, with a value of 10.2 g O_2/L-h. This observed peak pattern, in which the OUR peaks prior to the end of fermentation, is characteristic of *P. pastoris* growth (Wollborn et al., 2022). We ultimately use this maximum value to design the dimensions of the overall bioreactor. We also use the maximum OUR in phase 1 (3.2 g O_2/L-h) and phase 2 (3.7 g O_2/L-h) to design their respective operating conditions.

$$\text{Equation B1-12. } OUR = \frac{1}{Y_{X/O_2}}\frac{dX}{dt}$$

Figure B1-4

Oxygen Utilization Rate for R104
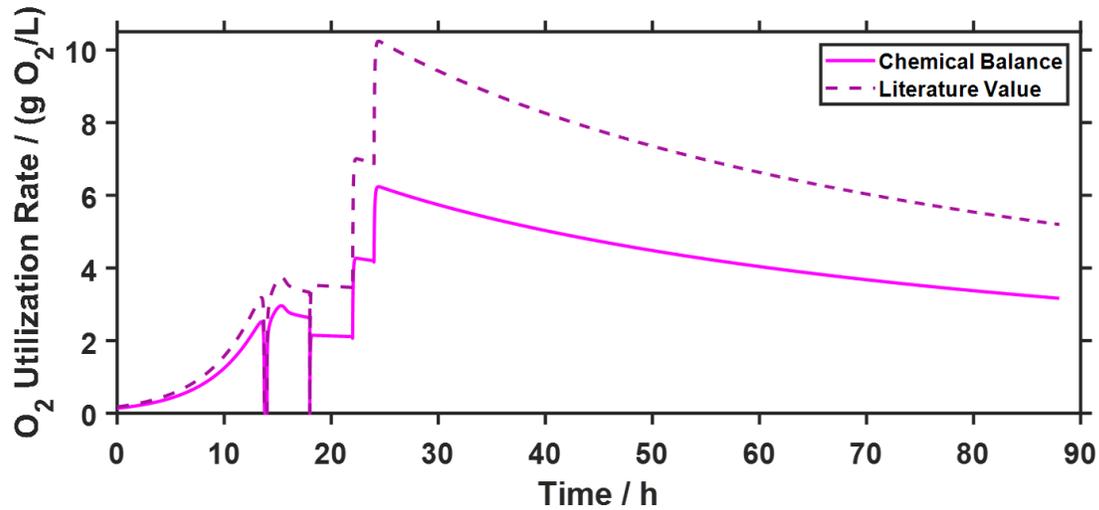
For our bioreactor, the rate of O_2 that we supply must be comparable to the rate of O_2 required by the yeast cells. The mass transfer coefficient (kLa) to meet this O_2 requirement is defined by Equation B1-13, where C^*_{O2} (g/L) is the solubility of O_2 in the media and C^{crit}_{O2} (g/L) is the critical concentration of dissolved oxygen that is required by cells. We estimate this value to be approximately 20% of C^*_{O2}. Given our OUR_{max} of 10.2 g O_2/L-h and that C^*_{O2} is 7.6 mg O_2/L at 30℃ (The Engineering ToolBox, 2005d), the target $k_L a$ is 1685 h^{-1}.

$$\text{Equation B1-13. } k_L a = \frac{OUR_{max}}{C^*_{O2} - C^{crit}_{O2}}$$

To find the optimal bioreactor dimensions and setup, we varied the working tank height (H_t [m]), tank diameter (D_t [m]), O_2 flow rate in the form of dry air (Q_g [m^3/h]), and impeller speed (N [rpm]) iteratively and solving Equations B1-(14-20) until the $k_L a$ calculation in Equation B1-13 matched that in B1-18, within 5% error. We also attempted to minimize the total reactor height, including headspace and gassed volume ($H_{t, tot}$ [m]), to ensure that the reactor is

not too large. In these equations, D_i is impeller diameter (m), which is approximately one-third of D_t, n_i is the number of impellers, ρ is bioreactor cell slurry and is approximately 1050 kg/m³ (Malairuang et al., 2020), μ is fluid viscosity and is approximately 0.18 kg/m-s (Global Pumps, n.d.). V is the final working volume of the tank (m³) and N_a is the aeration number. The power number (N_p) and (P_g/P) values were found via plotted correlations with Re and N_a, respectively. P and P_g are the power of ungassed and gassed systems, respectively, and A_t is the area cross section of the tank (Prpich, 2021a).

$$\text{Equation B1-14. } \frac{H_t - D_i}{D_i} > n_i > \frac{H_t - 2D_i}{D_i}$$

$$\text{Equation B1-15. } Re = \left(\frac{N}{60}\right)\frac{D_i^2 \rho}{\mu}$$

$$\text{Equation B1-16. } N_a = \frac{\left(\frac{Q_g V}{60}\right)}{\left(\frac{N}{60}\right)D_i^3}$$

$$\text{Equation B1-17. } P_g = \left(\frac{P_g}{P}\right)n_i N_p \rho \left(\frac{N}{60}\right)^3 D_i^5$$

$$\text{Equation B1-18. } k_L a = \left(\frac{0.0333}{D_t^4}\right)\left(\frac{P_g}{P}\right)^{0.541}\left(\frac{Q_g V}{60}\right)^{0.541/\sqrt{D_t}}$$

$$\text{Equation B1-19. } \phi = (1.8)\left(\frac{P_g}{V\mu}\right)^{0.14}\left(\frac{Q_g V}{60A_t}\right)^{0.75}$$

$$\text{Equation B1-20. } H_{t, tot} = (1.1)H_t(1 + \phi)$$

Ultimately, we determined that overall bioreactor dimensions are $H_{t, tot}$ = 5.1 m, D_t = 1.25 m, D_i = 0.42 m, and Q_g = 27 m³/h of dry air 20°C. In addition, we will use four baffles and three 6-blade Rushton impellers, with a spacing of 0.42 m. Bioreactor operation will include the use of single-use fermentation bags. For phase 1 of growth, we will operate at 300 rpm, with a power of 6.0 kW. For phase 2 of growth, we will operate at 340 rpm, with a power of 8.5 kW. For both of

these phases, only one impeller, positioned 0.5 m above the bottom of the tank, will be in use.

For phase 3 of growth, the impeller will be shifted down to 0.45 m above the bottom so that two

of the three impellers are completely submerged prior to the addition of MeOH. After 47.5 hours,

the bioreactor will temporarily be halted and the impellers will be shifted down to 0.42 m above

the bottoms so that all three impellers are completely submerged. This stepping of the impeller

will avoid any harmful shearing effects of an impeller intersecting with the fluid level. For this

phase, we will operate at 465 rpm, with a power of 115.6 kW.

1.4 Upstream Yield & Time Length

Overall, we assume 100% recovery of R21c by the end of upstream, and that we output

256 g R21c per batch. In total, the upstream portion of a batch takes 128 hours, or ~5.3 days

(Figure D4-1). According to downstream and formulation & fill-finish recovery (Section B2 and

B3), this necessitates 13 batches annually to meet our desired R21c demand.

2. Downstream

2.1 Centrifugation #1

The first step in the downstream process is to separate the *P. pastoris* cells from the rest

of the fermentation broth. From the final fermentation step, 2230 L of fluid from the production

bioreactor is fed into the first centrifuge. This slurry contains 300 kg of *P. pastoris*, which holds

256 g of unreleased R21c. We will use the AlfaLaval BTUX 305 system (Table B2-1), which

empties the entire bowl while simultaneously running an automated CIP (clean-in-place)

procedure, for centrifugation (*AlfaLaval BTUX 305*, 2018). This centrifuge has a maximum

throughput capacity of 2500 L/h and may be operated in the the range of 6000-9650 RPM. To

prevent overworking the centrifuge and promote better separation, we will operate at a feed rate

of 2,000 L/hr and a speed of 9500 RPM. As a result, the first centrifuge step will take 1.12 hours to process the fluid volume. The built-in CIP and SIP (sterilization-in-place) procedures involve 30 minutes of steam exposure, as well as an intermittently operating peripheral discharge solids-ejecting system, which requires 0.35 L of a caustic solution after each batch (*AlfaLaval BTUX 305*, 2018). Since these procedures take place during centrifugation downtime, they do not contribute to the final batch time calculation. The centrifuge will also require 1000 L/hr of cooling water to prevent the overheating of frame parts and seals during operation.

Table B2-1

Centrifuge Technical Specifications

Model	AlfaLaval BTUX 305
Throughput Capacity	2500 L/hr
Solids Handling	800 L/hr
Bowl Volume	3.1 L
Bowl Speed	9500 RPM
Motor Power	7.5 kW

We assume that in running the first centrifuge step, we will recover 98% of the cells in the solid phase entering the high pressure homogenizer. This solid phase will include 295 L of fluid so that the cells may flow smoothly out of the centrifuge in a slurry composition of 50 wt% cells. The remaining 1936 L of fluid will leave the system as overflow, along with the remaining 2% cells. At the end of the first centrifugation step, we expect to retain 294 kg of cells and 251 g of R21c, at a recovery of 98%, in the process.

<u>2.2 High Pressure Homogenization (HPH)</u>

Following the first centrifuge, the slurry is resuspended in approximately 995 L of pichia lysis buffer (PLB; Table H8), resulting in a total of 1290 L of solution running through the HPH step. This resuspension allows us to operate within the parameters of the homogenizer, as well as to ensure that the working volume of solution entering the future depth filtration step is 1000 L. The HPH apparatus applies pressure on the solution, and through shear force and turbulence, ruptures cell walls, ultimately lysing the yeast cells and releasing the R21c proteins, which are not secreted during protein production. We assume that these released fusion proteins spontaneously assemble into the final R21c VLP structure (K. A. Collins et al., 2017). At this point in the process, we will assume that the assembled particle is pure and the subsequent purification processes will only remove external impurities.

For this step, we will use the Ariete NS3037 Homogenizer for the cell lysing process. The homogenizer will run at a pressure of 1000 atm and has a feed flow rate of 1200 L/hr, with other operating specifications outlined in Table B2-2 (*Ariete NS3037*, 2010). This apparatus includes homogenizing valves that are designed for easy integration with maintenance and CIP procedures which will take approximately 2 hours to complete after each batch. We will cycle the slurry through the equipment twice to ensure that a high fraction of cells are lysed. The solution will also be cooled, via 90 L/h of cooling water, throughout HPH operation to ensure that heat released via apparatus operation does not denature the R21c proteins. We will assume that the two cycles of homogenization will release 90% of the protein. Thus, we estimate that 226 g of the protein will be released into solution during this step. In addition, at the specified flow rate, we expect each cycle to take 1.07 hours, for a total of 2.15 hours of operation.

Table B2-2

Homogenizer Technical Specifications

Model	Ariete NS3037
Pressure	1,000 bar
Flow Rate	1,200 L/hr
Motor Power	37 kW
Time per Cycle	1.07 hr
Cycles	2

2.3 Centrifugation #2

 Another centrifugation step must be performed on the entering 1290 L of solution in order to separate out cell debris from the desired protein. The same centrifuge model will be used for this centrifugation step (Table B2-1), and the apparatus will be operated with the same operating parameters (feed flow rate of 2000 L/hr and speed of 9500 RPM). Additionally, the cooling and CIP/SIP procedures are the same as in centrifugation #1, including 30 minutes of steam exposure and an intermittently operating peripheral discharge solids-ejecting system. Unlike in the first centrifugation step, we will be collecting the supernatant for further purification as the R21c VLPs will be suspended in solution. Using the same recovery of 98%, we estimate 221 g of the VLP will be suspended, and recovered, in the liquid phase following the centrifugation. The total volume of the liquid phase proceeding to depth filtration will be 1000 L. Under the operating conditions, we expect that this centrifugation step will take 0.64 hours.

2.4 Depth Filtration

Depth filtration must be performed to remove larger impurities, like whole yeast cells and cell debris, from the solution. This step is necessary at the beginning of purification to reduce the load and chance of fouling on later equipment from the presence of large molecules. Depth filters are composed of a porous medium made of tightly packed fibers. The tightly packed fibers only allow particles under the desired pore size to flow through. The larger particles are retained within the fibrous structure due to the tortuous and channel-like medium. Retention in the fibrous structure rather than on the surface prevents surface buildup and increases the recovery of the smaller molecules. Cellulose-based depth filters, which are able to remove significant amounts of DNA, host cell proteins, and viruses in addition to whole yeast cells (Cervera et al., 2019), have previously been used to process R21c in lab-scale studies (Mukhopadhyay et al., 2022).

For this step, Millistak+ HC Pod Depth Filter, a cellulose-based filter, will be used. The model offers single use disposable filters that have a surface area of 1.1 m^2. For operation, the manufacturer recommends a flow rate ranging from 40 to 109 L/min and a differential pressure of 10 psi (Millipore, 2019). We assumed a minimum yield of 90% at these operating conditions. Using the flow rate of 41.6 L/min and working volume, 1000 L, we estimated that the process time for this step would be 24 minutes. Here, we assume no volume lost during depth filtration.

2.5 Ultrafiltration

To reduce the volumetric load during Size-Exclusion Chromatography and Affinity Chromatography, batch ultrafiltration is required to concentrate the protein solution after depth filtration. The filter chosen for ultrafiltration is the single-use Sartocon® Self Contained Filter with a membrane area of 3.5 m^2. The filter has a nominal molecular weight cutoff of 300 kD, and since the R21c has a molecular weight of 4000 kD, it was assumed that most of the protein

26

would be retained in the retentate (Mukhopadhyay et al., 2022). Additionally, it was assumed the buffer would completely flow through the filter since the buffer molecules are significantly smaller than the molecular weight cutoff. The optimal ultrafiltration flux was assumed to be 85 L/m²·h and by multiplying the membrane area, the permeate flow was found to be 297.5 L/hr (Gil Dhawan, 1985). Since the filter operates in crossflow, the filter is resistant to fouling.

Following depth filtration, the protein is suspended in 1000 L of solution at a concentration of 0.199 g/L. To reduce the load during chromatography purification steps, the solution must be reduced to 100 L. Using this information, we can determine a concentration factor (CF):

$$\text{Equation B2-1. } CF = \frac{V_0}{V}$$

where V_0 and V are the initial volumes of the working solution.

Using CF = 10, we can calculate the final concentration of R21c in solution:

$$\text{Equation B2-2. } c = c_0 \cdot (CF)^{\sigma}$$

where c_0 and c are the initial and final concentrations, respectively, (g/L), and σ is the protein rejection coefficient. Even though R21c protein should be retained due to the large difference in nominal weight cut off, a conservative value of 0.95 was used based on data from proteins with comparable sizes (*Filter-Loop-Assembly*, 2016). The final concentration of R21c exiting UF will be 1.79 g/L.

$$\text{Equation B2-3. } t = \frac{V_0 - V}{A \cdot J_{AVG}}$$

We calculated processing time for the ultrafiltration step using Equation B2-3, where t is the process time (h), A is the membrane area (m³), and J_{AVG} is the average flux. The average flux

was used because it was assumed there was no build-up of protein on the membrane surface and so flux can be estimated as constant. The process time was found to be 3.03 hours.

2.6 Capto Core 700 Resin & Size-Exclusion Chromatography

Following ultrafiltration, chromatography will be performed using Capto Core 700 shell resins to remove smaller impurities. This technology utilizes an adsorbent core surrounded by an inert porous shell, which allows smaller impurities to bind to the internalized ligands while the larger desired product cannot (Figure B2-1). Capto Core combines size-exclusion and binding chromatography into one resin, resulting in the potential for a higher sample load and higher flow rates than in traditional size exclusion chromatography (*Capto Core 700*, n.d.; Mi et al., 2022). Based on existing data for Capto Core 700 models, we estimate that recovery of R21c protein in this step will be approximately 80% (Lagoutte et al., 2016; Shen et al., 2015).

Figure B2-1

Cross-section of Capto Core Illustrating Resin Shell Function
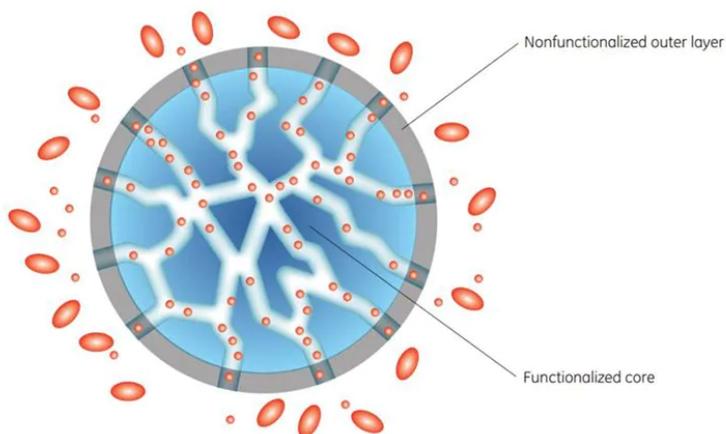
Note. Figure retrieved from (*Capto Core 700*, n.d.)

We will use a Capto Core 700 model in accordance with existing research on R21c VLP purification (Mukhopadhyay et al., 2022). Since DNA is negatively charged and the octalymine ligand core is positively charged at a pH below 10.5 (Mi et al., 2021), Cytiva recommends operating the resin at a pH range of 7-9 to remove DNA and host cell protein contaminants (Cytiva, 2020b). The residence time should be greater than 2 minutes as evidence shows that time frame is effective at removing contaminants 5 nm in diameter or below (Mi et al., 2021). Similar experimentation on R21c purification using a Capto Core chromatograph operated at a flow rate of 20 mL/min corresponds to a flow velocity of 61.1 cm/hr (Mukhopadhyay et al., 2022).

For our proposed process design, we will upscale the lab scale equipment to a 20 liter ReadyToProcess model produced by Cytiva (Cytiva, 2023). The 20 L Capto Core will be operated at the same flow velocity as it is recommended to remain constant at scale-up (Cytiva, 2020b). The 20 liter column has dimensions of 359 mm in diameter and 200 mm in height which leads to a residence time of 19.6 minutes (Cytiva, 2020a)**.** The specifications for the ReadyToProcess model and operating conditions are displayed in Table B2-3. The Capto Core column will be operated using the AKTA Ready XL single-use chromatography system, also developed by Cytiva. This system is designed for manufacturing scale chromatography and allows for the flow rates required for this process (*AKTA Ready XL*, n.d.).

Table B2-3

Capto Core 700 Design Specifications

Column dimension	359 mm ID, 200 mm H
Column volume (CV)	20 L
Flow velocity	61.1 cm/h
Flow rate	1.03 L/min

All specifications from Cytiva, 2023; Mukhopadhyay et al., 2022.

Although the ReadyToProcess models are designed as single use columns, research demonstrates that they may be operated, under proper conditions, for up to 50 trials without the binding capacity degrading (Cytiva, 2018)**.** Therefore, we will use only one Capto Core model annually as we are only operating 13 batches per year. Based on this research, recommendations from Cytiva, and the necessary volume throughput for the column, we determined the quantity of the solutions for each step (Table B2-4) in Capto Core operation (Cytiva, 2020a; Mukhopadhyay et al., 2022). Wash, CIP, and Sanitization step operating parameters are derived from those suggested in the ReadyToProcess columns User Manual from Cytiva (Cytiva, 2020b). The process time for the flow through of the desired product is 1.64 hours. The total time for Capto Core chromatography, including equilibration, wash, CIP, and SIP, is 6.54 hours, but these additional steps will only be run during Capto Core downtime and thus will not contribute to overall batch scheduling.

Table B2-4

Capto Core 700 Operation Specifications

Step	Stream #[1,2]	Volume	Step Time (min)	Composition
Equilibrate	2110	3 × CV	58.9	10 mM Tris 1 mM MgCl$_2$ 1 mM EDTA 0.1% Triton
Load Sample	In: 2100 Out: 2160	5 × CV	98.2	172.1 g R21c 10 mM Tris 1 mM MgCl$_2$ 1 mM EDTA 0.1% Triton
Wash	2120	6 × CV	117.8	H$_2$O
CIP	2130	3 × CV	58.9	1 M NaOH in 30% Isopropanol
Sanitization	2140	3 × CV	58.9	0.5 M NaOH

1. Figure 4
2. All input streams except for the eluted load sample leave as waste in stream 2150

All values from Cytiva, 2020a; Mukhopadhyay et al., 2022.

2.7 Affinity Chromatography

Affinity chromatography is performed to further separate the R21c fusion protein from contaminants, mainly AOX 1. We chose CaptureSelect™ C-tagXL Affinity Matrix created by Thermo Fisher Scientific. The affinity matrix ligand is a fragment of a Camelid antibody that selectively binds to the E-P-E-A peptide (C-tag) on R21c, offering high selectivity (Thermo Fisher Scientific, 2017). To design the affinity chromatography process, we scaled-up from lab-scale separations by maintaining residence time. The lab-scale residence time was five minutes, calculated with Equation B2-4 (Mukhopadhyay et al., 2022). Given the limits of readily available chromatography columns and resin specifications, we calculated a residence time of six minutes for our column by adjusting column height and flow velocity accordingly. For our

equipment, we chose a Chromaflow chromatography column made by Cytiva based on the apparatus' usage recommendation for process scale biopharma production and its capacity for clean-in-place operations. The specifications for our chosen chromatography column and affinity matrix are described in Table B2-5.

$$\text{Equation B2-4. } residence\ time\ (min)\ =\ \frac{flow\ velocity\ (cm/hr)}{column\ height\ (m)}\ \times\ 100\ (\tfrac{m}{cm})\ \times\ 60\ (\tfrac{min}{hr})$$

Table B2-5

Affinity Chromatography Design Specifications

Column dimensions	400 mm ID, 200 mm H
Column volume (CV)	25.1 L
Flow velocity	200 cm/hr
Flow rate	4.2 L/min
Resin dynamic binding capacity	400 nmol/mL

Columns specifications from Cytiva, n.d.; Resin/flow specifications from Thermo Fisher Scientific, 2017

The column is packed according to the resin manufacturer's specifications for flow packing. Recommendations suggest that flow packing be performed at 150% of the process operating flow rate (Thermo Fisher Scientific, 2015). The amount of slurry required is determined by the manufacturer's formula (Equation B2-5), where the suggested slurry ratio is 0.5 and packing factor is 1.17. The resulting slurry for our column is estimated to be 58.8 L. Based on the slurry volume and flow velocity, the column will be packed over 0.35 hour (21 minutes). This time is outside of the scope of batch scheduling. Other affinity chromatography resins by the same manufacturer have life cycles of over 100 uses, so we will assume that our resin will not require a change during the production cycle (*MabCaptureC Protein A*

Chromatography Resin, n.d.). We will completely empty our column of resin once production is complete for the year and then re-pack the column just prior to the next production period.

$$\text{Equation B2-5. } slurry\ volume\ required\ (L)\ = \frac{column\ volume\ (L)}{slurry\ ratio} \times packing\ factor$$

In order to meet our production goal, we estimated, based on estimated protein recoveries throughout the manufacturing process, that we would need 141 g of R21c entering our column per batch. Based on upstream production, preceding downstream recoveries and concentration of the sample in ultrafiltration, the actual protein concentration with our proposed design from the Capto Core 700 is 1.43 g/L. Using Equation B2-6, we determined the necessary volume of filtrate from the Capto Core was 100 L to allow for 143 g R21c to appropriately enter the column.

$$\text{Equation B2-6. } volume\ in\ (L)\ = \frac{protein\ demand\ (g)}{concentration\ in\ (g/L)}$$

In each batch, the chromatography process involves seven steps. The first equilibration step is performed to prepare the column for elution by creating the optimal binding environment between the affinity matrix and the C-tag on the VLP. Next, the sample, which is the filtrate from the previous Capto Core step, is loaded into the column. The wash step is performed with the sample buffer to encourage non-binding particles to elute. The first elution step creates conditions that will cause binding of the AOX 1 to the resin to be unfavorable. The next elution step, a much higher salt buffer, causes the binding of the C-tag to the resin to become unfavorable, resulting in R21c elution. Next, the column is re-equilibrated before being cleaned or stripped by continuously cycling the cleaning solution through the system for a period of time.

This completes one cycle. The operating specifications and stream table for this process are listed in Table B2-6 and D3-3.

Table B2-6

Affinity Chromatography Operating Specifications

Step	Stream #[1,2]	Volume	Step time (min)	Composition
Equilibrate	2170	$10 \times CV^3$	60	20 mM Tris
Load sample	2160	129.5 L	24	143 g R21c 10 mM Tris 1 mM $MgCl_2$ 1 mM EDTA 0.1% Triton
Wash	2180	$5 \times CV$	30	10 mM Tris 1 mM $MgCl_2$ 1 mM EDTA 0.1% Triton
Elute contaminants	2190	$5 \times CV$	30	20 mM Tris 0.1 mM $MgCl_2$
Elute R21c	In: 2200 Out: 2230	$5 \times CV$	30	122 g R21c 20 mM Tris 2 mM $MgCl_2$
Re-equilibrate	2170	$5 \times CV$	60	20 mM Tris
Strip	2210	$2.5 \times CV$	15	500 mM citric acid

1. Figure 4
2. All input streams except for the eluted R21c leave as waste in stream 21
3. CV = column volume

All values from Thermo Fisher Scientific, 2017

Equation B2-7. $step\ time\ (min)\ =\ \frac{volume\ to\ load\ (L)}{flow\ rate\ (L/min)} +\ residence\ time\ (min)$

With our chosen flow rates and volumes of fluid, the entire affinity chromatography cycle for one batch will take 4.9 hours (Table B2-6, Equation B2-7). However, the equilibration and stripping steps will not extend the downstream process time as they can be performed while the

R21c sample is passing through other manufacturing steps. Thus, the contribution by affinity

chromatography to the overall process time is 1.9 hours or 114 minutes. In total, the column will

send 5 CV, 125.7 L, to the next step and recover 85% of the protein passed through for a total of

122 g of R21c (Jin et al., 2017).

2.8 Diafiltration

After affinity chromatography, the working volume is 125.7 L, with a protein

concentration of 0.95 g/L. Before sterile filtration, the product must be exchanged from the

chromatography buffer to WFI. Using the same single-use Sartocon® Self Contained Filter

model used in the ultrafiltration step, we will operate the feed flow rate at 297.5 L/h, the same as

the ultrafiltration permeate flow rate, to maintain a constant volume process. To determine the

total volume of WFI used during diafiltration, we used:

$$\text{Equation B2-8. } \left(\frac{C}{C_0}\right) \ = \ exp(-\frac{v_w}{v_0} \cdot (1 - \sigma_{buffer}))$$

where C and C_0 are the initial concentrations of buffer removed (g/L), respectively, v_w is the total

volume of WFI added (L), v_0 is the volume to be diafiltered (L), and σ_{buffer} is the rejection

coefficient of the buffer, assumed to be 0 due to the small molecular weight. Assuming 99%

removal of the previous buffer species, 578 L of WFI are needed for a constant media volume of

125.7 L. We calculate the processing time for this step (Equation B2-9) as 1.95 hours.

$$\text{Equation B2-9. } t \ = \ \frac{v_w}{A \cdot J_{AVG}}$$

Due to the large difference in size between filter pore size and the R21c protein, we

assumed most of the protein would be retained during diafiltration. Using the filter specification

sheet, we used a conservative retention of 97% of the protein. This results in an R21c

concentration of 0.922 g/L.

2.9 Intermediate Mixing Tank

To minimize the risk of contamination in the final product, the WFI based solution will be diluted after diafiltration and before sterile filtration. To fill the vials with 5 μg of R21c with the minimum volume before lyophilization, 0.2 mL, the desired filling concentration is 0.025 g/L. However, to account for protein loss in the vial filling and lyophilization steps, we must instead dilute the solution to 0.027 g/L. To achieve this concentration, 4230 L of WFI will be added in an intermediate mixing tank to produce a final volume of 4355 L. This mixing step will take 2.11 hours. Specific tank design is considered in Section C2.

2.10 Sterile Filtration

Sterile filtration is the last step before the formulation of the product. The presence of viruses in biopharmaceuticals can pose a significant risk to patient safety, as some viruses can cause disease. Sterile filtration is performed in order to remove remaining bacteria, viruses, and undesired microorganisms, as well additional yeast protein contaminants, from the R21c solution. This process works by passing the liquid through a membrane filter that is designed to remove particles of a certain size. We chose to use a Charged Durapore® Optiseal® Cartridge Filter with a small pore size of 0.22 microns and an area of 2.07 m^2. This filter is made from polyvinylidene fluoride membrane that has been modified to have a net positive charge (Millipore, 2023). The charged membrane will be able to separate negatively charged endotoxins from the solution, regardless of their size (Millipore, 2023). Since the R21c molecules are 22 nm in diameter, they will freely pass through the membrane while it retains the larger viral particles. The filter will be used with a recommended flow rate of 2500 L/hr. The resulting processing time is 1.74 hours.

One of the main challenges with sterile filtration is the potential for the filter membrane to become clogged. This can occur if the liquid being filtered has a large number of contaminant particles or if the liquid passes through the membrane at a high flow rate. The filtration steps preceding sterile filtration will help to prevent the filter becoming clogged with an abundance of viral particles, but maintenance and membrane replacement will be required from time to time. The filtration must also be performed in a clean environment in order to minimize the risk of contamination of the filter membrane. When these measures are taken to ensure that the process runs efficiently, the theoretical yield from this step of the downstream process will be 100%.

2.11 Downstream Recovery & Time Length

In considering the recovery at every major downstream step, we determine that we have 46% recovery efficiency (Table B4-1). By producing 3.30 kg R21c from upstream per year, we will surpass our annual production goal by producing enough R21c for 21,776,975 vaccines, a surplus of ~853,900 vaccines. The total time of all downstream processes is approximately 16.7 hours (Figure D4-2).

3. Formulation and Fill-Finish

3.1 Vial Filling

For vial filling, we will use the SA25 Aseptic Filling Workcell, which is an automated vial filler produced by Cytiva. This workcell can fill about 20,000 vials per pass, which takes approximately 45 minutes with unloading. To meet filling demand for lyophilization, we will use 4 SA25 workcells to process 364,000 vials in 3.4 hours (t), as calculated via Equation B3-1:

$$\text{Equation B3-1. } t = \frac{Rv}{n}$$

where R is rate of vial filling (Cytiva, 2022), v is the number of vials to be filled per batch, and n is the number of SA25 Aseptic Filling Workcells. The minimum possible automated vial filling volume is 0.2 mL per vial. Operating at the minimum volume specifications allows us to run vial filling for less time. In addition, lyophilization will be quicker as there will be less liquid to evaporate. Assuming some spillage, the vial filling step will produce an R21c yield of 95%.

3.2 Lyophilization

The next step in the process is lyophilization. We will be freeze-drying R21c for improved stability and preservation during storage. We will be using two QuantaS™ Steam Sterilizable Production Freeze Dryers that can each lyophilize 182,000 vials in 3 hours. Following the recommended 10 hour sterilization and down time, the lyophilizers will only run 3 cycles a day, thus processing 1,092,000 vaccines per day. Therefore, to process all 21,776,975 vials, we will need 20 days for filling and lyophilization. Starting a new batch every 20 days will allow the filling and lyophilization of vaccines to be essentially continuous throughout our yearly operation cycle. Despite the very long filling and lyophilization time, our operation would only run 266 days a year due to the small amount of batches needed. Lyophilization has a recovery of 97% (Czyż & Pniewski, 2016). As a result, we expect 5 µg of R21c per vial.

3.3 Matrix-M Addition & Administration

A Matrix-M adjuvant will be mixed with the R21c protein directly before the vaccine is administered. R21c must be stored at -80℃ and Matrix-M must be stored at 2-8℃ with protection from light (Datoo et al., 2022). Therefore, it is imperative that they be kept separate throughout the entire shipping and storage procedures. This process is not in the scope of our project, as the adjuvant will be purchased from NovaVax and the final formulation will be

performed at time of injection. Vaccine reconstitution will involve mixing 0.5 mL of Matrix-M

(0.1 g/L) with the R21c VLPs in the vials. This produces a 0.5 mL vaccine, with the appropriate

5 µg R21c to 50 µg Matrix-M ratio, that will be administered via an intramuscular injection in

the arm (University of Oxford, 2023).

4. Overall Protein Recovery Efficiency & Purity

In considering the recovery at every major downstream and formulation & fill-finish step,

we determine that we have 43% recovery efficiency (Table B4-1). As a result, to meet demand,

we will need to produce at least 246 g R21c per batch in our upstream process. With our

proposed design, we exceed our demand by expecting to produce 256 g of R21c in the upstream

process. Overall, we expect to produce 21,776,975 vaccines per batch while producing 13

batches annually.

A comparable process for lab-scale production of the VLP achieved a >98% purity using

the CaptureSelect C-tag affinity resin for the affinity chromatography step. With the use of the

improved resin, CaptureSelect C-tagXL Affinity Matrix, Jin et al. yielded >99% purity for a

different malaria vaccine when also used with tangential flow filtration and size exclusion

chromatography (2017). Because we utilize each of those methods, we also expect to achieve

>99% purity throughout our downstream purification process.

Table B4-1

Incremental Process Recovery Efficiency

Stage	Recovery	Cumulative Recovery	Amount of R21c Protein Out (g)	Time (hours)
Upstream	100%	100%	255.9	128
Centrifugation #1	98%	98%	250.8	1.12
High Pressure Homogenization	90%	88%	225.7	2.15
Centrifugation #2	98%	86%	221.2	0.64
Depth Filtration	90%	78%	199.1	0.40
Ultrafiltration	90%	70%	179.2	3.03
Capto Core 700	80%	56%	143.3	1.64
C-Tag Purification	85%	48%	121.8	1.90
Diafiltration	97%	46%	118.1	1.95
Mixing Tank	100%	46%	118.1	2.11
Sterile Filtration	100%	46%	118.1	1.74
Fill-Finish	95%	44%	112.2	480
Lyophilization	97%	43%	108.9	

High pressure homogenization recovery from Zhang et al., 2019
Ultrafiltration recovery from *Filter-Loop-Assembly*, 2016
Capto Core 700 recovery from Lagoutte et al., 2016; Shen et al., 2015
C-Tag Purification recovery from Jin et al., 2017
Lyophilization recovery from Czyż & Pniewski, 2016

C. Ancillary Equipment

1. Cooling Jacket

Most protocols for *P. pastoris* fermentation discuss the use of cooling jackets since there is a narrow temperature range (28-32 °C) in which the yeast is viable (Invitrogen, 2002; Stratton et al., 1998). As a result, we calculated heat generation in our production bioreactor, R104, as described by Equation C1-1, in which $Y_{Q/O2}$ (kJ/g) is the yield coefficient for heat production from O_2 consumption. For this heat generation calculation, we used the literature calculated values for OUR to have conservative estimates. In addition to considering the heat of reaction, calculating the amount of heat that must be transferred to our cooling liquid depends on the amount of heat required to warm the entering air feed to the reactor temperature and vaporize a portion of the water. As a result, we use Equation C1-2 to calculate the total heat that must be transferred throughout the production bioreactor run (Figure C1-1). Here, m_s (kg/h) is the mass flow rate of the media formulations, $m_{O2,in}$ (kg/h) is the mass flow rate of O_2, and $m_{N2,in}$ (kg/h) is the mass flow rate of N_2 into the bioreactor. $m_{O2,out}$ (kg/h) is the mass flow rate of O_2, $m_{N2,out}$ (kg/h) is the mass flow rate of N_2, and $m_{CO2,out}$ (kg/h) is the mass flow rate of CO2 out of the bioreactor. $m_{xsH2O(l)}$ (kg/h) is the mass accumulation rate of byproduct in the bioreactor and $m_{xsH2O(g)}$ (kg/h) is the mass flow rate of vaporized H_2O into the leaving gas stream. $C_{p,s}$ (4.18 kJ/kg*K), $C_{p,O2}$ (0.918 kJ/kg*K), $C_{p,N2}$ (1.04 kJ/kg*K), $C_{p,CO2}$ (0.849 kJ/kg*K), and $C_{p,H2O}$ (4.18 kJ/kg*K) are the specific heat capacities of the media, O_2, N_2, CO_2, and H_2O (The Engineering ToolBox, 2005c, 2005b, 2005a). $\Delta H_{vap,H2O}$ (2429.8 kJ/kg) is the heat of vaporization of water at 30°C and 1 atm (The Engineering ToolBox, 2010). T_S, T_{air}, and T_{out} are the temperatures of the entering substrate streams (30°C), entering air stream (20°C), and final temperature of all contents in the bioreactor (30°C). T_{ref} (30°C) is the reference temperature for calculations. This

allows us to simplify Equation C1-2 to Equation C1-3. The sustained heat generation at ~44 kW suggests that the temperature in the bioreactor will rise significantly, and thus we must design a cooling jacket to keep the yeast healthy and productive.

$$\text{Equation C1-1. } Q_{rxn} = OUR * V * Y_{Q/O2}$$

Equation C1-2.

$$Q_t = m_s C_{p,s}(T_S - T_{ref}) + m_{O2,in} C_{p,O2}(T_{air} - T_{ref}) + m_{N2,in} C_{p,N2}(T_{air} - T_{ref}) + Q_{rxn}$$

$$- m_{O2,out} C_{p,O2}(T_{out} - T_{ref}) - m_{N2,out} C_{p,N2}(T_{out} - T_{ref}) - m_{CO2,out} C_{p,CO2}(T_{out} - T_{ref})$$

$$- m_{xsH2O(l)} C_{p,H2O}(T_{out} - T_{ref}) - m_{xsH2O(g)} \Delta H_{vap,H2O}$$

Equation C1-3.

$$Q_t = m_{O2,in} C_{p,O2}(T_{air} - T_{ref}) + m_{N2,in} C_{p,N2}(T_{air} - T_{ref}) + Q_{rxn} - m_{xsH2O(g)} \Delta H_{vap,H2O}$$

Figure C1-1

Rate of Heat to be Removed from R104
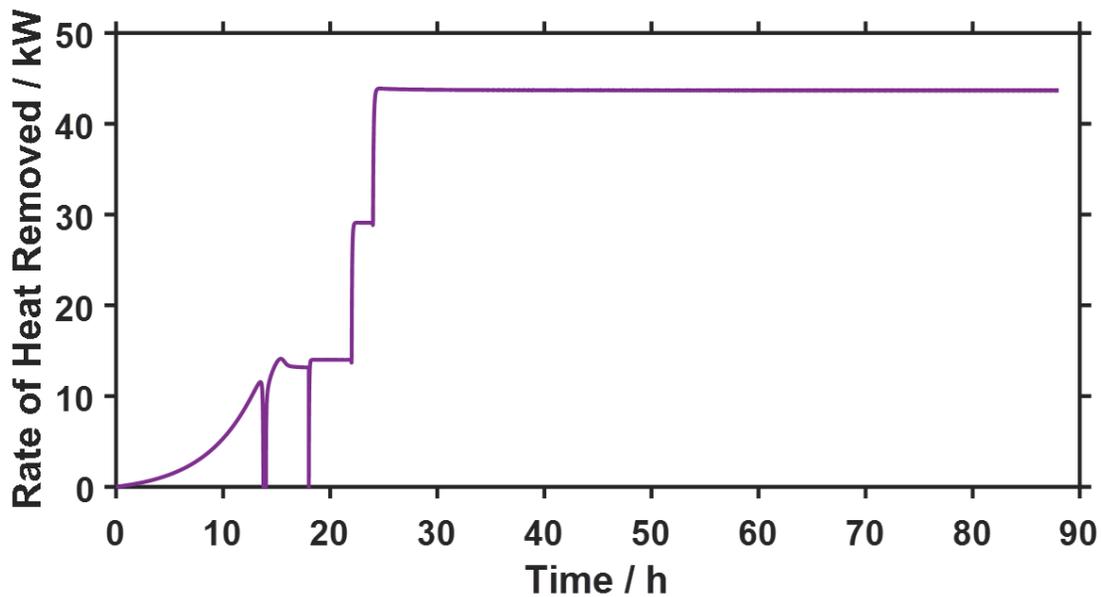
To confirm that a cooling jacket is feasible for the dimensions of our tank, we calculated the minimum necessary jacket area to dissipate the heat (A_o [m^2]) with Equations C1-(4-9). Here, ΔT_{lm} (°C) is the logarithmic mean temperature difference between the bioreactor and cooling water streams, $T_{cool,out}$ (25°C) is the final temperature of the cooling water leaving the reactor, and $T_{cool,in}$ is the initial temperature of the cooling water entering the reactor. Pr is the dimensionless Prandtl number for the fluid inside the bioreactor, k is the thermal conductivity of fluid (0.6132 W/m*K), Nu_i is the dimensionless Nusselt number for the fluid in the agitated tank, and a (0.54) and b (⅔) are the Nu_i parameters for tanks with rushton impellers. h_i is the internal convective heat transfer coefficient and U_o is the overall heat transfer coefficient. In our calculations, we set U_o to be equivalent to h_i as we assume that external convective heat transfer and conductive heat transfer through the reactor walls is negligible (Carta, 2021). We compared the resulting A_o values to the surface area of the bioreactor walls covered by fermentation broth (A_{wall}) with Equation C1-10, in which H_l is the height of the fluid in the tank (m). By testing different inlet water temperatures, we find that $T_{cool,in}$ = 9°C is the highest temperature at which $A_o < A_{wall}$ throughout the production bioreactor's operation and the cooling jacket is feasible for our tank dimensions (Figure C1-2).

$$\text{Equation C1-4. } m_{EG,cool} = \frac{Q_t}{C_{p,EG}(T_{cool,out} - T_{cool,in})}$$

$$\text{Equation C1-5. } \Delta T_{lm} = \frac{(T_{out} - T_{cool,out}) - (T_{out} - T_{cool,in})}{ln((T_{out} - T_{cool,out})/(T_{out} - T_{cool,in}))}$$

$$\text{Equation C1-6. } Pr = \frac{\mu * C_{p,H2O}}{k}$$

$$\text{Equation C1-7. } Nu_i = a * Re^b * Pr^{1/3}$$

$$\text{Equation C1-8. } U_o = h_i = \frac{Nu_i * k}{D_t}$$

$$\text{Equation C1-9. } A_o = \frac{Q_t}{U_o * \Delta T_{lm}}$$

$$\text{Equation C1-10. } A_{wall} = \pi D_t H_l$$

Figure C1-2

Comparison of the Minimum Required for Cooling and Actual R104 Tank Surface Area
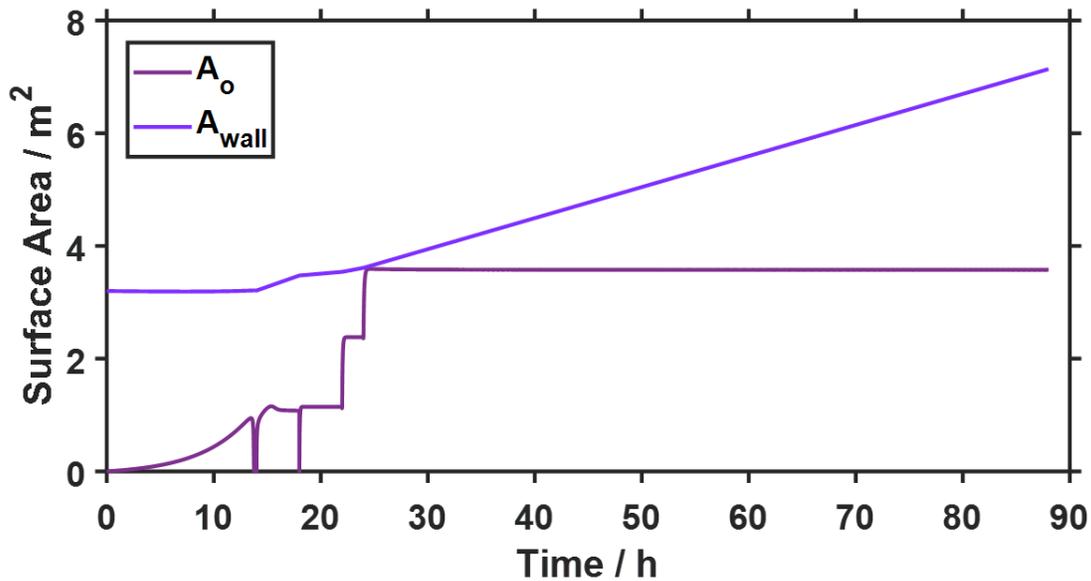
Since the cooling jacket is feasible for our reactor dimensions, we will design the jacket to be 1-2 mm in thickness, surrounding the wall of the bioreactor. For the coolant in our cooling jacket, we will use 9°C 60 wt% ethylene glycol that will be heated to 25°C via the net heat generated in the bioreactor. Using Equation C1-4, we calculated the mass flow rate of the water through the jacket ($m_{EG,cool}$ [kg/h], Figure C1-3), in which $C_{p,EG}$ (3.249 kJ/kg*K) is the specific heat capacity of the 60 wt% ethylene glycol (The Engineering ToolBox, 2003). A total of 208500 kg of coolant will be used during one run of the production bioreactor.

Figure C1-3

Mass Flow Rate of Ethylene Glycol through the R104 Cooling Jacket
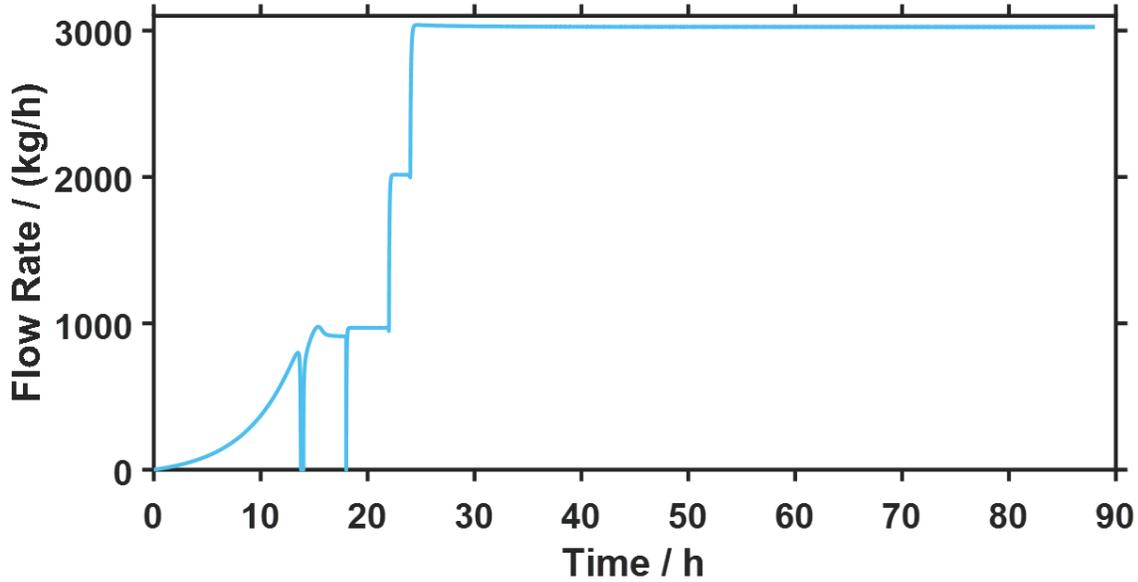
2. Tanks

Cylindrical tanks with a vertical orientation are utilized throughout the production process to store intermediate chemical solutions, buffers, and media required for each step. In order to ensure a homogeneous mixture and prevent settling and swirling, these tanks will be agitated with baffles. The size of each tank is determined based on the quantity of its respective components needed in all stages of development. We estimated the cost of the tanks by sourcing existing pharmaceutical mixing tanks online and scaling them to the appropriate size required for this process based on demand. We determined the power requirement for each tank with the same method for calculating reactor power in the upstream process. Since these tanks are ungassed, we adjusted Equation B1-17 as follows:

$$\text{Equation C2-1. } P = n_i N_p \rho \left(\frac{N}{60}\right)^3 D_i^5$$

3. Pumps

Fluid transport between production process steps requires the use of pumps. Peristaltic pumps are the preferred choice throughout production due to their ability to handle a wide range of flow rates, maintain high purity and sterile solutions, accommodate slurries and viscous solutions, and offer low maintenance costs. The purchase and utility costs of each pump were determined based on the required flow rate and power input. To ensure consistency and flexibility in the plant, only Masterflex L/S, I/P, and B/T models, which offer flow rates ranging from 0.036 to 42 L/min, will be utilized throughout the process (*Masterflex Peristaltic Pumps and Fluid Handling Solutions*, 2023). Additionally, using three models from one company's design for all pumps allows for easy repairs with interchangeable parts. We expect to purchase spare parts for each model. In our proposed process, all streams flowing into vessels require pumps to transport the fluids. However, some waste streams flowing out do not require pumps as they already have enough momentum, generated from the equipment or previous pump, to flow.

$$\text{Equation C3-1. } P_P = \Delta P \cdot Q$$

To determine the operating costs associated with the pumps used throughout the process, we calculated the power requirement for each of the pumps used in the process (Equation C3-1). The power is determined in Watts by multiplying the differential pressure (ΔP [Pa]) by the volumetric flow rate (Q [m³/s]). Differential pressures were chosen based on the pressure necessary across the membranes in different vessels. If there was no pressure difference across the unit, a differential pressure of 1 atm was assumed. We also assumed frictional losses in each tube are equal to 0.5 atm. We did not use gravity head in our calculations as there are no

significant changes in height throughout the process. The pumps were assumed to be 70%

efficient in order to calculate the power requirement in operating costs.

D. Final Recommended Design

1. Process Flow Diagrams & Equipment Tables

Figure D1-1

Upstream Process Flow Diagram for Proposed R21c Manufacturing Process
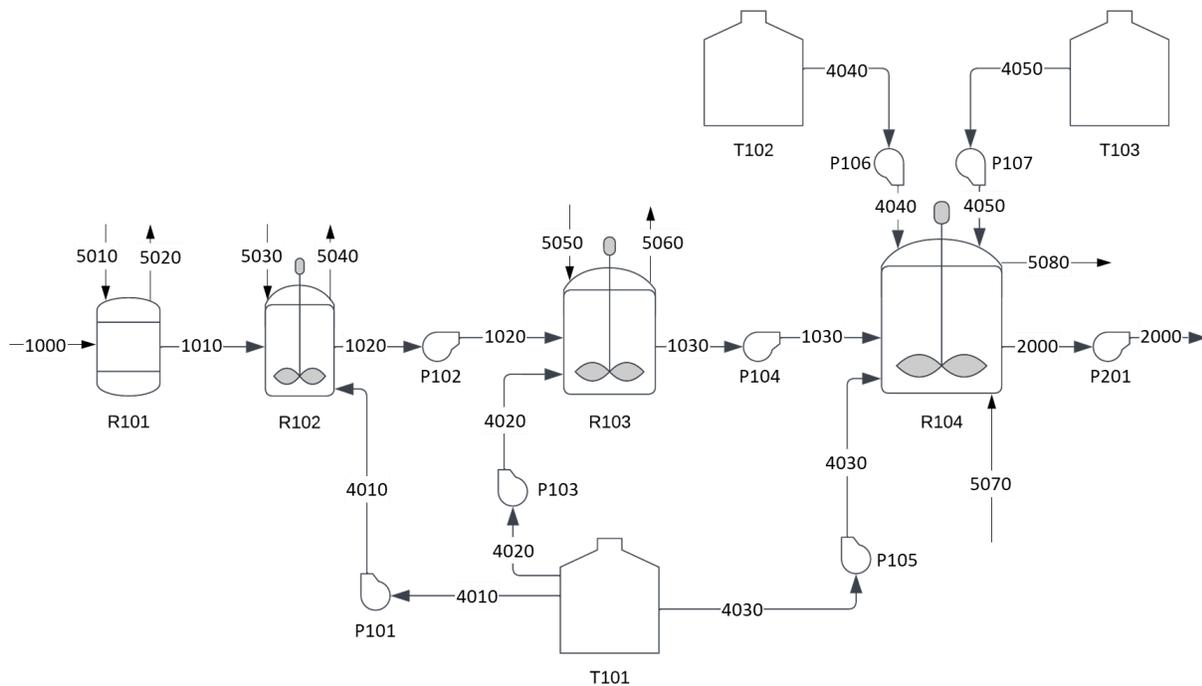
Note. FS111, A112, WC113, and WH114 are not explicitly included in the diagram as they are

not a part of the main process flow.

Figure D1-2

Downstream Process Flow Diagram for proposed R21c manufacturing process
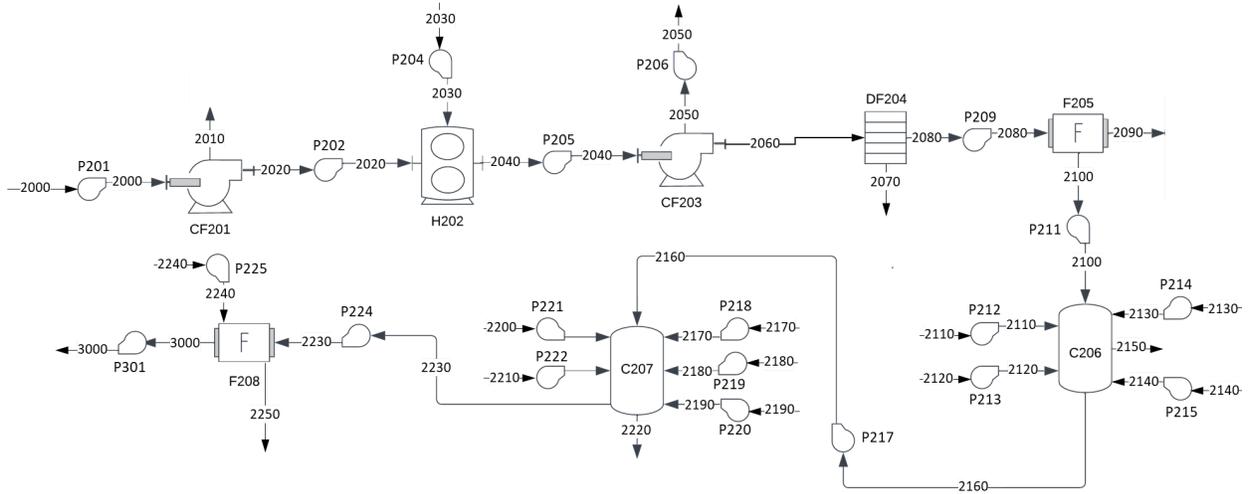
Note. Ancillary tanks are not explicitly included in the diagram. Refer to Table D1-2 for tank locations.

Figure D1-3

Formulation & Fill-Finish Process Flow Diagram for proposed R21c manufacturing process
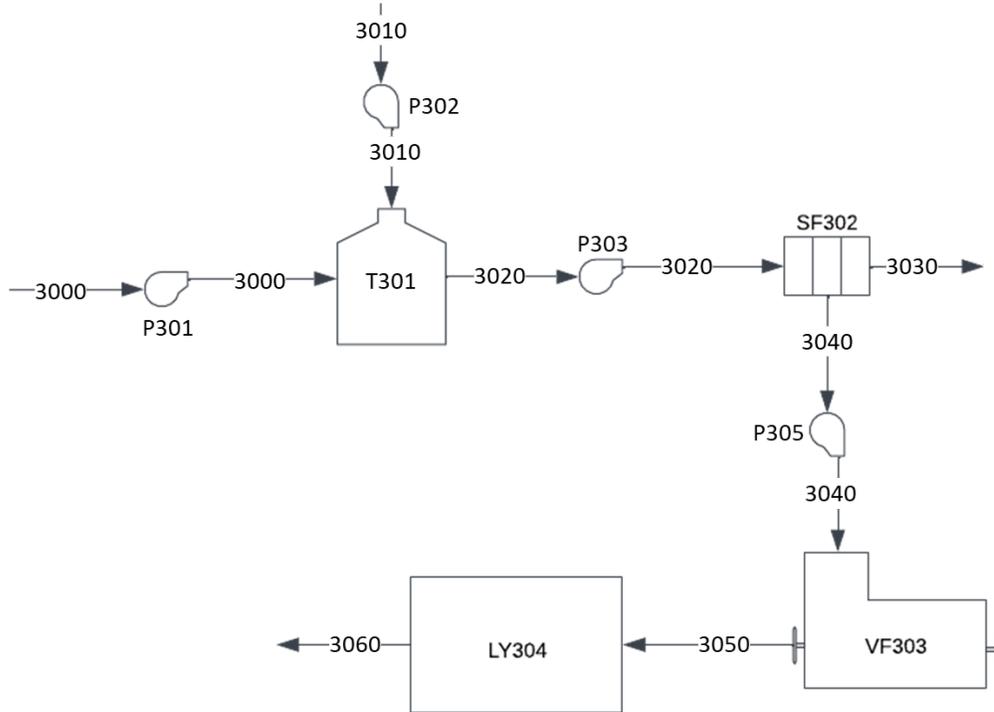
Note. Sterile filtration is considered as a part of downstream but will be considered in

Formulation & Fill-Finish for accounting purposes.

Table D1-1

Major Equipment Table for R21c Production Process

Equipment	Name	Recovery	Cumulative Recovery	Time (hours)
R101	250 mL Shake Flask	100%	100%	9.5
R102	2.5 L Bioreactor	100%	100%	16
R103	50 L Bioreactor	100%	100%	14.5
R104	Production Bioreactor	100%	100%	88
CF201	Centrifuge #1	98%	98%	1.12
H202	High Pressure Homogenizer	90%	88%	2.15
CF203	Centrifuge #2	98%	86%	0.64
DF204	Depth-Filtration	90%	78%	0.40
F205	Ultrafiltration	90%	70%	3.03
C206	Capto Core 700	80%	56%	1.64
C207	Affinity Chromatography	85%	48%	1.90
F208	Diafiltration	97%	46%	1.95
T301	Mixing Tank	100%	46%	2.11
SF302	Sterile Filtration	100%	46%	1.74
VF303	Vial Filling	95%	44%	480
LY304	Lyophilization	97%	43%	

Table D1-2

Ancillary Tanks used in R21c Production Process

Location	Components	Equipment Name	Stream
2.5 L Bioreactor	Glycerol Media	T101	4010
50 L Bioreactor	Glycerol Media	T101	4020
Production Bioreactor	Glycerol Media	T101	4030
	Glycerol Fed-batch Media	T102	4040
	Methanol Fed-batch Media	T103	4050
HPH	PLB Buffer Solution	T201	2030
Capto Core	Equilibration Buffer	T202	2110
	CIP Buffer	T203	2130
	Sanitization Buffer	T204	2140
Affinity Chromatography	Equilibration Buffer	T205	2170
	Loading Buffer	T206	2180
	Elute Contaminants Buffer	T207	2190
	Elute R21c Buffer	T208	2200
	Stripping Buffer	T209	2210
Diafiltration	Buffer	T210	2240

Table D1-3

Pumps used in R21c Production Process

Location	Description	Equipment Name	Stream
2.5 L Bioreactor	Cell Media to Reactor	P101	4010
50 L Bioreactor	Cell Culture to Reactor	P102	1020
	Cell Media to Reactor	P103	4020
Production Bioreactor	Cell Culture to Reactor	P104	1030
	Glycerol Batch to Reactor	P105	4030
	Glycerol Feed to Reactor	P106	4040
	Methanol to Reactor	P107	4050
Centrifugation 1	Slurry to Centrifuge	P201	2000
HPH	Slurry to Homogenizer	P202	2020
	PLB Buffer Solution	P204	2030
Centrifugation 2	Slurry to Centrifugation	P205	2040
	Centrifuge Waste	P206	2050
Ultrafiltration	Product to UF	P209	2080
Capto Core	Product to Capto Core	P211	2100
	Equilibration Pump	P212	2110
	Wash Pump	P213	2120
	CIP Pump	P214	2130
	Sanitization Pump	P215	2140

Affinity Chromatography	Product to Affinity Chromatography	P217	2160
	Equilibration Pump	P218	2170
	Wash Pump	P219	2180
	Elute Contaminants Pump	P220	2190
	Elute Protein Pump	P221	2200
	Stripping Pump	P222	2210
Diafiltration	Product to DF	P224	2230
	Buffer to DF	P225	2240
Mixing Tank	Product to tank	P301	3000
	WFI to Tank	P302	3010
Sterile Filtration	Product to SF	P303	3020
Vial Filling	Product to VF	P305	3040

2. Stream Tables

Table D2-1

Upstream Stream Compositions and Volumes

Stream	Description	Material	Amount/batch
1000	Inoculum to R101	Master Seed (CBF) Yeast cells MGY media Pure glycerol	1 mL 0.25 g 250 mL 2.5 g
5010	Air Feed to R101	O_2 N_2	3.80 g 12.6 g
5020	Waste Gas from R101	CO_2 N_2 O_2 H_2O	0.830 g 12.6 g 3.01 g 0.442 g
1010	Cell Culture to R102	Yeast cells Broth	1.75 g 251 mL
4010	Media Feed to R102	Basal Salts media Pure glycerol	2.25 L 90.0 g
5030	Air Feed to R102	O_2 N_2	64.0 g 211 g
5040	Waste Gas from R102	CO_2 N_2 O_2 H_2O	29.9 g 211 g 35.5 g 7.35 g
1020	Cell Culture to R103	Yeast cells Broth	55.7 g 2.53 L
4020	Media Feed to R103	Basal Salts media Pure glycerol	47.5 L 1.90 kg
5050	Air Feed to R103	O_2 N_2	1.16 kg 3.83 kg
5060	Waste Gas from R103	CO_2 N_2 O_2 H_2O	630 g 3.83 kg 558 g 133 g

1030	Cell Culture to R104	Yeast cells Broth	1.20 kg 50.6 L
4030	Media Feed to R104 for Glycerol Batch Phase (1)	Basal Salts media Pure glycerol	949 L 3.80 kg
4040	Media Feed to R104 for Glycerol Fed-Batch Phase (2)	Glycerol feed Pure glycerol	76.9 L 35.9 L
4050	Media Feed to R104 for MeOH Fed-Batch Phase (3)	MeOH feed Pure MeOH	727 L 569 kg
5070	Air Feed to R104	O_2 N_2	634 kg 2090 kg
5080	Waste Gas from R104	CO_2 N_2 O_2 H_2O	338 kg 2090 kg 140 kg 68.3 kg
2000	Fermentation Contents Entering Downstream	Yeast cells Pure glycerol Pure MeOH R21c Broth	300 kg 128 g 75.9 g 256 g 2230 L

Table D2-2

Downstream Stream Compositions and Volumes

Stream	Description	Material	Amount/batch
2010	Waste Stream from CF201	Broth Yeast cells Unreleased R21c	1936 L 6.00 kg 5.12 g
2020	Cell Slurry to H202	Broth Yeast cells Unreleased R21c	294 L 294 kg 250.7 g
2030	Buffer Addition to H202	PLB	994 L
2040	Lysed Solution to CF203	PLB + Broth Yeast cells Released R21c Unreleased R21c	1288 L 294 kg 225.7 g 25 g
2050	Waste Stream from CF203	PLB + Broth Yeast cells Released R21c Unreleased R21c	288 L 288 kg 4.5 g 25 g
2060	R21c Solution to DF204	PLB + Broth Yeast cells Released R21c	1000 L 5.88 kg 221.2 g
2070	Waste from DF204 Filter Change	R21c in Filter	22.1 g
2080	R21c Solution to F205	R21c PLB	199 g 1000 L
2090	Waste from F205	R21c PLB	19.6 g 900 L
2110	Equilibrate to C206	Tris $MgCl_2$ EDTA Triton WFI	73 g 6 g 18 g 15 mg 60 L

2100	Load Sample to C206	R21c Tris MgCl$_2$ EDTA Triton WFI	172 g 121 g 10 g 29 g 25 mg 100 L
2120	Wash to C206	WFI	120 L
2130	CIP to C206	NaOH in 30% Isopropanol	60 L
2140	Sanitization to C206	NaOH	61.2 kg
2170	Equilibrate to C207	Tris WFI	1.2 kg 251 L
2160	Load Sample to C207	R21c Tris MgCl$_2$ EDTA Triton WFI	143 g 121 g 10 g 29 g 25 mg 100 L
2180	Wash (PLB) to C207	Tris MgCl$_2$ EDTA Triton WFI	1.2 kg 12 g 37 g 32 mg 126 L
2190	Contaminant Elution Buffer to C207	Tris MgCl$_2$ WFI	304 g 1.2 g 126 L
2200	Elute Contaminants from C207	Tris MgCl$_2$ WFI	304 g 24 g 126 L
2210	Stripping Solution to C207	Citric acid WFI	6 kg 63 L
2230	Eluted R21c Product to F208	R21c Tris MgCl$_2$ WFI	122 g 0.3 kg 24 g 126 L
2240	WFI to F208	WFI	579 L
2250	Waste from F208	R21c Tris MgCl$_2$ WFI	3.7 g 3 g 24 g 705 L
3000	Product Entering Formulation and Fill-Finish (T301)	R21c WFI	118 g 126 L

Table D2-3

Formulation & Fill-Finish Compositions and Volumes

Stream	Description	Material	Amount/batch
3010	WFI to T301	WFI	4230 L
3020	Diluted Product to SF302	R21c WFI	118 g 4355 L
3030	Waste from SF302	Other protein	*Specific amount not accounted for throughout process*
3040	Sterile Product to VF303	R21c WFI	118 g 4355 L
3050	Vials to LY304	R21c Inactivated R21c WFI Vials	112 g 6 g 4140 L 21776975 Vials
3060	Product	R21c Inactivated R21c Vials	109 g 9 g 21776975 Vials

3. R21c VLP Process Parameters and Operation

3.1 250 mL Shake Flask

A 1 mL vial of frozen cells, obtained from CBF, should be thawed to inoculate 250 mL of MGY media in a 1 L Corning® Erlenmeyer cell culture flask. The flask will spend 9.5 hours on a rotary shaker, after which the cell concentration will increase from 1 g/L to 6.99 g/L and the substrate will be fully consumed. After the fermentation step, the contents of 250 mL shake flask are poured into the 2.5 L bioreactor (R102). The flasks will be autoclaved and cleaned with detergent after use.

3.2 2.5 L Bioreactor

The shake flask contents are emptied into 2.25 L of Basal Salts media held in the Allegro™ XRS 25 Bioreactor System. Batch fermentation will occur for 16 hours, during which time dry air is fed in at a rate of 0.015 m^3/h. After fermentation, the cell concentration will be 22.1 g/L and the substrate will be fully consumed. The contents of the 2.5 L bioreactor are then pumped into the 50 L bioreactor (R103). The single-use fermentation bag will be discarded and replaced after use.

3.3 50 L Bioreactor

The 2.5 L bioreactor contents are emptied into 47.5 L of Basal Salts media held in the Allegro ™ STR Single-use Stirred Tank Bioreactor. Batch fermentation will occur for 14.5 hours, during which time dry air is fed in at a rate of 0.30 m^3/h. After fermentation, the cell concentration will be 23.6 g/L and the substrate will be fully consumed. The contents of the 50 L bioreactor are then pumped into the production bioreactor (R104). The single-use fermentation bag will be discarded and replaced after use.

3.4 Production Bioreactor

The 50 L contents are emptied into 949 L of Basal Salts media held in the production bioreactor. All relevant reactor dimensions and operating parameters are listed in Table D3-1. The height of the lowest impeller will be positioned 0.5 m from the bottom of the tank for the first 18 hours of fermentation. The height will be decreased to 0.45 m for the next 29.5 hours, and then to 0.42 m for the remainder of the fermentation. At the end of the process, the concentration of yeast cells is 135 g/L and 156 g of R21c are produced. The final concentrations

of glycerol and methanol are negligible in the fermentation broth. The single-use fermentation

bag will be discarded and replaced after use.

Table D3-1

Reactor Dimensions and Operating Conditions for Production Bioreactor (R104)

Parameter	Value
Tank Height	5.1 m
Tank Diameter	1.25 m
Type of Impeller	6-blade Rushton
Number of Impellers	3
Baffles	4
Working Volume Range	1000 - 2230 L
Aeration Rate (dry air 20°C)	27 m^3/h
Phase 1: Glycerol Batch Growth	
Gassed Power Requirement	6.0 kW
Maximum Impeller Speed	300 rpm
Feed Type	Basal Salts
Fermentation Time	14 hours
Phase 2: Glycerol Fed-Batch Growth	
Gassed Power Requirement	8.5 kW
Maximum Impeller Speed	340 rpm
Feed Type	Glycerol Feed
Feed Flow Rate	18.15 L/h
Fermentation Time	4 hours

Phase 3: Methanol Fed-Batch Growth	
Gassed Power Requirement	115.6 kW
Maximum Impeller Speed	465 rpm
Feed Type	Methanol Feed
Feed Flow Rate	3.6 L/h (t < 4 h) 7.3 L/h (4 h < t < 6 h) 10.9 L/h (t > 6 h)
Fermentation Time	70 hours

3.5 Centrifuge #1

Following fermentation, the yeast cells containing the R21c proteins must be separated

from the rest of the fermentation broth using the AlfaLaval BTUX 305 centrifugation system. In

this step, the feed enters the centrifuge at a feed rate of 2000 L/h and is processed with a

rotational speed of 9500 RPM. The resulting processing time is 1.12 hours and the retained yeast

cell slurry consists of 50 wt% cells in leftover fermentation broth. This slurry contains 98% of

the cells and 251g of R21c produced during fermentation. CIP and SIP times are not explicitly

allocated for this step, but the procedure will take approximately 30 minutes during centrifuge

downtime.

3.6 High Pressure Homogenizer

After collecting the yeast cells, the slurry is resuspended in 995 L of PLB, for a total of

1290 L of solution. The Ariete NS3037 Homogenizer will lyse the cells by operating at 1000 atm

and a feed flow rate of 1200 L/h. Each cycle of the homogenizer takes 1.07 hours, and with two

cycles per batch, the homogenizer will operate for a total of 2.15 hours. With an efficiency of

90%, 226 g of R21c will be released, and spontaneously assembled into VLP form. The

homogenization step will spend approximately 2 hours on CIP and SIP procedures during HPH downtime.

3.7 Centrifuge #2

Following cell lysis, a second centrifugation step will be used to remove the majority of cellular debris from the desired protein in solution using the same AlfaLaval BTUX 305 model centrifuge. In this step, the feed will again enter the centrifuge at a feed rate of 2000 L/h and be processed at a rotational speed of 9500 RPM. The resulting time is 0.64 hours and the retained yeast cell slurry consists of 50 wt% cells in leftover fermentation broth. This slurry contains 98% of the cells (lysed and unlysed) and 221g of released R21c leaving the homogenizer. CIP and SIP times are not explicitly allocated for this step, but the procedure will take approximately 30 minutes during centrifuge downtime.

3.8 Depth Filtration

Depth filtration is performed to remove larger impurities, like whole yeast cells and cell debris, in the solution in order to reduce the load on later equipment. For this step, Millistak+ HC Pod Depth Filter, a cellulose based filter, will be used. The model offers single use disposable filters that have a surface area of 1.1 m^2. For yield, the manufacturer's recommended flow rate of 41.6 L/min and a differential pressure of 10 psi will be used. For yield, a minimum yield of 90% was assumed at these operating conditions. Overall, the time to process the working volume of 1,000 L will be 24 minutes.

3.9 Ultrafiltration

To reduce the volumetric load during chromatography steps, batch ultrafiltration with the single-use Sartocon® Self Contained Filter, having a membrane area of 3.5 m^2 and a nominal

molecular weight cutoff of 300 kD, will be used to concentration the protein solution after depth

filtration. The volume of the solution will be reduced to 100 L and concentration of R21c in the

liquid will change from 0.199 g/L to 1.79 g/L. Operation at the optimal ultrafiltration flux of 85

$L/m^2 \cdot h$ gives a permeate flow of 297.5 L/hr. This step will take 3.03 hours.

3.10 Capto Core 700 Size-Exclusion Chromatography

The 20L ReadyToProcess Capto Core 700, prepacked with resin, will be used to capture

impurities smaller than R21c via a multimodal method. The R21c protein will elute through the

column while impurities such as DNA fit through the pores and bind to internalized ligands. The

process requires five column volumes for the R21c sample load. The equilibration, CIP, and

sanitization each require three column volumes of PLB, 1 M NaOH in 30% isopropanol, and 0.5

NaOH, respectively. The wash step requires six column volumes of WFI. The operating

parameters and dimensions of the column are listed in Table D3-2. The total R21c solution

volume will be maintained and the concentration will decrease to 1.43 g/L.

Table D3-2

Dimensions and Operating Conditions for Capto Core 700 (C206)

Column dimension	359 mm ID, 200 mm H
Column volume (CV)	20 L
Flow velocity	61.1 cm/h
Flow rate	1.03 L/min
Residence time	19.6 min
Resin	ReadyToProcess Capto Core 700
Estimated recovery	80%
Process time	1.64 hr
Equilibration to CIP (full cycle) time	6.55 hr

All specifications from Cytiva, 2023; Mukhopadhyay et al., 2022.

3.11 Affinity Chromatography

The CaptureSelect™ C-tagXL Affinity Matrix column has high selectivity for the C-tag on the R21c fusion protein, making it an advantageous step in protein purification and recovery. Table D3-3 lists column dimensions and operating parameters. All resin specifications, including flow, volume and packing velocity came from the resin manufacturer, Thermo Fisher Scientific (2017). The eluted R21c solution will be 125.7 L in volume at a concentration of ~0.97 g/L.

Table D3-3

Dimensions and Operating Conditions for C-tag Affinity Chromatography (C207)

Column dimensions	400 mm ID, 200 mm H
Column volume (CV)	25.1 L
Flow velocity	200 cm/hr
Flow rate	4.2 L/min
Resin	CaptureSelect™ C-tagXL Affinity Matrix
Resin dynamic binding capacity	400 nmol/mL
Resin packing flow velocity	300 cm/hr
Resin slurry required	58.8 L
Resin estimated recovery	85%
Resin packing time	0.35 hr
Process time	1.9 hr
Equilibration to CIP (full cycle) time	4.9 hr

Columns specifications from Cytiva, n.d.; Resin/flow specifications from Thermo Fisher Scientific, 2017

3.12 Diafiltration

After Affinity Chromatography, the working volume of 125.7 L will pass through ultrafiltration with a single-use Sartocon® Self Contained Filter (membrane area of 3.5 m^2 and a nominal molecular weight cutoff of 300 kD) for a buffer exchange a buffer exchange from the chromatography buffer to WFI. To maintain constant volume during the process, the feed flow rate of WFI is the same as the ultrafiltration permeate flow rate of 297.5 L/hr. Assuming 99% removal of the previous buffer species, 578 L of WFI will be cycled through during diafiltration and the final R21c solution will be 125.7 L at 0.922 g/L. The processing time is 1.95 hours and R21c recovery will be 97%.

3.13 Intermediate Mixing Tank

To minimize the risk of contamination after sterile filtration, the WFI-based R21c
solution will be diluted in an intermediate mixing tank before sterile filtration. The tank will mix
4230 L of WFI to produce a final volume of 4355 L at a target concentration of 0.027 g/L. This
intermediate mixing step will take 2.11 hours. Tank operating specifications and dimensions are
listed in Table D3-4.

Table D3-4

Dimensions and Operating Conditions for Intermediate Mixing Tank (T301)

Tank Volume	5000 L
Impellers #	1
Impeller Type	Rushton
Impeller Diameter	0.618 m
Impeller Speed	100 RPM
Power Usage	2.58 kW

3.14 Sterile Filtration

Sterile filtration with a Charged Durapore® Optiseal® Cartridge Filter (0.22 μm pore
size and 2.07 m^2 area) removes any existing bacteria, viruses, undesired microorganisms, and
negatively charged endotoxins from the R21c solution. Operating at a flow rate of 2500 L/h, the
processing time is 1.74 hours. 100% R21c recovery and no volume change is expected during
this step.

3.15 Vial Filling & Lyophilization

Vial filling will be performed with four SA25 Aseptic Filling Workcells, allowing for 364,000 vials to be processed in 3.4 hours. The minimum possible automated vial filling volume of 0.2 mL per vial will be used to decrease lyophilization time.

Lyophilization via two QuantaS™ Steam Sterilizable Production Freeze Dryers will be able to lyophilize 364,000 vials in 3 hours. Following the recommended 10 hour sterilization and down time, the lyophilizers can only run 3 cycles a day, allowing for the daily production of 1,092,000 vaccines. In total, 20 days are needed to fill and lyophilize 21,776,975 vials. Vial filling and lyophilization will each have recoveries of 95% and 97%, respectively.

3.16 Vaccine Distribution, Storage, & Administration

The packaged R21c VLPs will be stored at -80℃ while distributing the vaccine from the plant in South Africa to distribution points across SSA. Matrix-M, acquired from NovaVax, will be stored at 2-8℃ under protection from sunlight. Immediately before injection, the 5 μg of R21c stored in a vial will be reconstituted with 0.5 mL of Matrix-M (0.1 g/L). The final vaccine will be administered intramuscularly in the arm.

4. Batch Production Schedule

Figure D4-3 depicts the overall process batch schedule for the production of R21c VLPs. Here, we block upstream (5.3 days, Figure D4-1), downstream (14.7 hours, Figure D4-2), and vial filling and lyophilization (20 days). To allow vaccine filling and lyophilization to be continuous throughout our yearly operation cycle, we will start a new batch every 20 days, for 13

batches. As a result, we will be operating for approximately 266 days, or ~8.9 months, every year. We intend to lease out our space and equipment to other companies and clinical trials during the remainder of the year when we are non-operational. However, we will not account for this additional revenue in our following economic analysis.

Figure D4-1

Upstream Batch Schedule
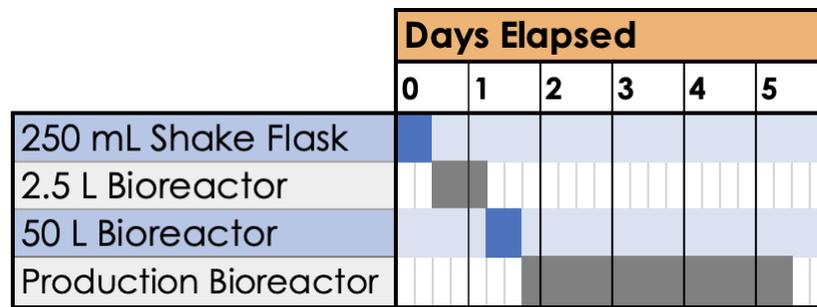
Figure D4-2

Downstream Batch Schedule
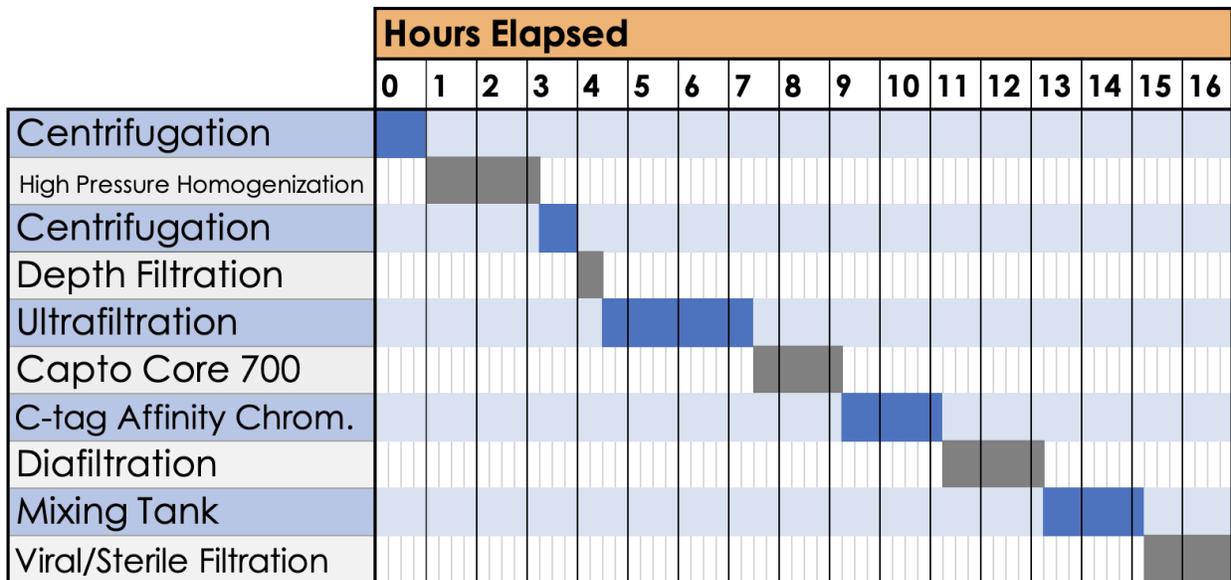
Figure D4-3

Overall Process Schedule
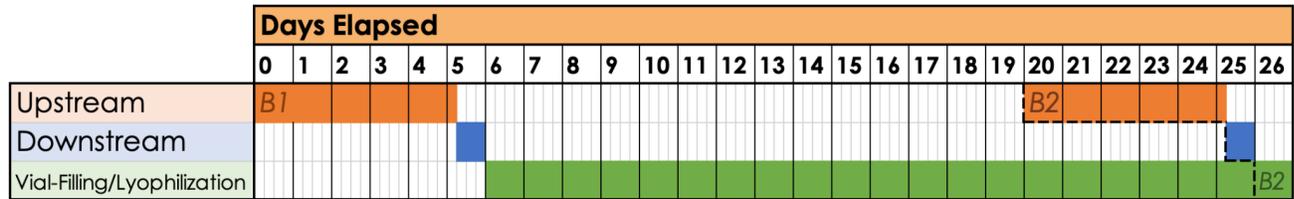
5. Economic Analysis

5.1 Capital Costs

We determine our capital costs from a variety of sources, including prices posted by manufacturers and those found in literature. To calculate the total cost associated with the purchase, transport, and installation of each piece of equipment, we used Wroth factors (Green & Southard, 2019). Multiplying the purchase cost of equipment with their corresponding Wroth factor, as well as an additional 5% cushion, yields a conservative estimate of the total cost of installing the equipment. Table D5-1 lists the purchase price and the installed cost of all the main equipment and ancillaries.

Table D5-1

Purchased and Installed Cost of Main & Ancillary Equipment

	Equipment Tag	Purchase Price	Wroth Factors	Installed Cost
Upstream				
Main Equipment				
1 L Shake Flask	R101	$29.84	2.5	$78.33
Flask Shaker	FS111	$2,287.56	2.5	$6,004.85
Autoclave	A112	$3,094.08	2.5	$8,121.96
2.5 L Bioreactor	R102	$5,100.00	2.5	$13,387.50

50 L Bioreactor	R103	$5,100.00	2.5	$13,387.50
Production Bioreactor (with cooling jacket)	R104	$27,100.00	2.5	$71,137.50
Water Chiller	WC113	$6,000.00	4.8	$30,240.00
Water Heater	WH114	$3,000.00	4.8	$15,120.00
Ancillaries				
Cell Media to Reactor Pump	P101	$5,450	5	$28,613
Cell Culture to Reactor Pump	P102	$5,450	5	$28,613
Cell Media to Reactor Pump	P103	$10,950	5	$57,488
Cell Culture to Reactor Pump	P104	$10,950	5	$57,488
Glycerol Batch to Reactor Pump	P105	$14,364	5	$75,411
Glycerol Feed to Reactor Pump	P106	$5,450	5	$28,613
Methanol to Reactor Pump	P107	$5,450	5	$28,613
Glycerol Batch Media Tank	T101	$1,625.00	4.1	$6,995.63
Glycerol Fed-batch Media Tank	T102	$592.00	4.1	$2,548.56
Methanol Fed-batch Media Tank	T103	$1,625.00	4.1	$6,995.63
Downstream				
Main Equipment				
Centrifuge	CF201	$100,000.00	2	$210,000.00
Homogenizer	H202	$125,000.00	2.5	$328,125.00
Centrifuge	CF203	$100,000.00	2	$210,000.00
Depth filtration System	DF204	$48,000.00	2.5	$126,000.00
Ultrafiltration filter loop	F205	$107,000.00	2.5	$280,875.00
AKTA Ready XL	C206	$215,000.00	2.5	$564,375.00
Diafiltration filter Loop	F208	$107,000.00	2.5	$280,875.00
Sterile filtration filter	SF209	$48,000.00	2.5	$126,000.00
Ancillaries				
Slurry to Centrifuge Pump	P201	$14,364	5	$75,411
Broth out of Centrifuge Pump	P202	$14,364	5	$75,411
Slurry to Homogenizer Pump	P203	$14,364	5	$75,411

PLB Buffer Solution Pump	P204	$14,364	5	$75,411
Slurry to Centrifugation Pump	P205	$14,364	5	$75,411
Centrifuge Waste Pump	P206	$14,364	5	$75,411
Product to Depth Filtration Pump	P207	$14,364	5	$75,411
Product to UF Pump	P208	$10,950	5	$57,488
Product to Capto Core Pump	P209	$5,450	5	$28,613
Equilibration Pump	P210	$5,450	5	$28,613
Wash Pump	P211	$5,450	5	$28,613
CIP Pump	P212	$5,450	5	$28,613
Sanitization Pump	P213	$5,450	5	$28,613
Product to Affinity Chromatography Pump	P214	$10,950	5	$57,488
Equilibration Pump	P215	$10,950	5	$57,488
Wash Pump	P216	$10,950	5	$57,488
Elute Contaminants Pump	P217	$10,950	5	$57,488
Elute Protein Pump	P218	$10,950	5	$57,488
Stripping Pump	P219	$10,950	5	$57,488
Product to DF Pump	P220	$10,950	5	$57,488
Buffer to DF Pump	P221	$10,950	5	$57,488
PLB Buffer Solution Tank	T201	$1,625	4.1	$6,996
Equilibration Buffer Tank	T202	$592	4.1	$2,549
CIP Buffer Tank	T203	$592	4.1	$2,549
Sanitization Buffer Tank	T204	$592	4.1	$2,549
Equilibration Buffer Tank	T205	$1,625	4.1	$6,996
Loading Buffer Tank	T206	$688	4.1	$2,962
Elution Buffer 1 Tank	T207	$688	4.1	$2,962
Elution Buffer 2 Tank	T208	$688	4.1	$2,962
Stripping Buffer Tank	T209	$592	4.1	$2,549
Diafiltration Buffer Tank	T210	$1,185	4.1	$5,101

Formulation and Fill-Finish				
Main Equipment				
Vial Filler	VF301	$532,000.00	2.5	$1,396,500.00
Vial Filler	VF301	$532,000.00	2.5	$1,396,500.00
Vial Filler	VF301	$532,000.00	2.5	$1,396,500.00
Vial filler	VF301	$532,000.00	2.5	$1,396,500.00
Lyophilization freeze dryer	LY302	$242,000.00	2.5	$635,250.00
Lyophilization freeze dryer	LY302	$242,000.00	2.5	$635,250.00
Ancillaries				
WFI to tank Pump	P301	$14,364	5	$75,411
Product to Tank Pump	P302	$10,950	5	$57,488
Product to SF Pump	P303	$14,364	5	$75,411
Product to VF Pump	P304	$14,364	5	$75,411
Mixing Tank	T301	$4,206	4.1	$18,107
Total Cost				**$11,935,554.65**

To calculate the total fixed capital of our plant, we used multiplicative factors. Multiplying the price of installed equipment by the multiplicative factors yields the remaining costs required to build the vaccine manufacturing plant (Green & Southard, 2019). We determined the finalized cost of our production scale plant using these multiplicative factors (Table D5-2).

Table D5-2

Capital Cost of R21c Manufacturing Plant

Category	Multiplicative Factor	Cost
Installed Equipment	1	$11,935,555
Piping	0.75	$8,951,666
Electrical/Instrumentation	0.3	$3,580,666
Buildings	0.5	$5,967,777
Yard Improvements	0.15	$1,790,333
Service Facilities	0.5	$5,967,777
Contingency	0.25	$2,983,889
Total Direct Costs		**$41,177,664**
Contracting	0.35	$4,177,444
Engineering	0.25	$2,983,889
Total Fixed Capital		**$48,338,996**

5.2 Operating Costs

      The yearly operating costs of the plant are made up of variable and fixed production costs that are required to run the processes. Variable costs include the cost of raw materials, waste treatment, and utilities. All raw materials are shown in Table D5-3 organized by process step.

Table D5-3

Annual Raw Material Usage

Materials	Annual Quantity	Annual Cost
Upstream		
Frozen Cells	13 vials (1 mL)	$260
Media and Substrate	Table H9	$150,044
2.5 L/50 L Fermentation Bags	26	$13,000
Production Scale Fermentation Bags	13	$13,000
WFI for CIP/SIP	6.5 L	$53
Downstream		
Depth Filtration Filter Cartridges	13	$10,751
UF Filter Cartridges	13	$2,600
Capto Core 700 Column	1	$96,511
Affinity Matrix	59 L	$473,629
DF Filter Cartridges	13	$2,600
Sterile Filtration Filter Cartridges	13	$20,878
Chromatography Column	1	$279
Media, Buffers, and CIP Chemicals	Table H10	$1,106,829
Formulation & Fill-Finish		
WFI	59,817 L	$478,535
Vials	283,100,675 vials	$33,972,081
Vial Stopper	283,100,675 stoppers	$28,310,068
Vial Seal	283,100,675 seals	$39,634,095
Matrix-M (0.1 g/L)	141,550 L	$70,775,169
Total Cost of Raw Materials		**$175,060,381**

The majority of raw material spending will go towards vial, vial stopper, and vial seals, which cover ~58.2% of the total raw material cost per year. Matrix-M accounts for ~40.5% of the total cost. Of the remaining 1.4% of raw material cost, the majority is taken up by substrates,

media, buffers, and CIP chemicals that will be used in the process. Another major contributor is the affinity matrix, which must be replaced once per year. In addition to considering raw materials in the manufacturing process, we also account for cost of waste disposal and utilities, which primarily includes electricity and ethylene glycol coolant.

Based on our operation schedule, we determined that our process will require six operator positions per shift. In accordance with the recommendation for five operators per shift position, we will have a total of 30 operators, each being paid $60,000/year, working in the plant . This allows for a four-shift rotation while also accounting for weekends, holidays, and vacations (Towler & Sinnott, 2012). In addition to operators, supervisors will be required to ensure that the plant runs efficiently. To cover each of the shifts, there will be six supervisors, each of whom will be paid $75,000/year in accordance with the recommendation that all combined supervisor salaries be 25% of all combined operator salaries (Towler & Sinnott, 2012). We will assume a salary overhead of 50% of total salary costs to account for training and benefits for employees. Maintenance and repair costs are valued at 3% of our inside battery limit investment and insurance is valued at 1% of our total fixed capital. Finally, corporate overhead charge was calculated as 65% of all labor costs to account for general and administrative costs (Towler & Sinnott, 2012). These costs are summarized in Table D5-4.

Table D5-4

Annual Plant Operating Costs

Category	Cost
Variable Production Costs	
Raw Materials Cost (Upstream)	$176,357
Raw Materials Cost (Downstream)	$1,714,077
Raw Materials Cost (Formulation & Fill-Finish)	$173,169,947
Waste Treatment	$8,000,024
Utilities	$3,360,808
Fixed Production Costs	
Labor Costs	$3,375,000
Maintenance and Repairs	$984,683
Insurance	$411,777
Corporate Overhead Charge	$2,193,750
Yearly Operating Costs	**$193,386,423**

5.3 Financial Viability of Plant

Under the previously outlined specifications, the plant will produce 283 million doses of

the R21c/Matrix-M vaccine, sold for $3 per dose, per year, resulting in a maximum expected

revenue of $849,300,000. However, this is ~11 million vaccines in surplus of our expected

demand. As a result, under given conservative conditions, we only expect to sell 272 million

doses and gain a revenue of $816,000,000. Although realistically we would drop our operating

costs to ensure we do not make too much surplus, under the operating parameters of our plant

design, this surplus is necessary, due to our batch schedule, to meet the expected demand.

Realistically, we expect to market the surplus to adults and people affected by malaria in other

regions of the world. However, for the purposes of our economic analysis, we will ignore this

additional revenue. In assessing plant economics, we expect that the construction and

implementation of all invested capital will take approximately one year (year 0). To assess the

financial viability of the proposed plant design, we will analyze a few potential operating

scenarios. For all following scenarios, we will model cash flow for 20 years of operation.

5.3.1 Scenario 1: Conservative Case

The conservative case scenario involves selling the expected demand quantity of

manufactured vaccines to SSA. Consistent positive net profit demonstrates clear profitability

(Table D5-4). Here, we assume a depreciation of 10% of the capital investment for 10 years,

afterwhich depreciation goes to $0. We also assume that taxes are 30%, accounting for federal

and state tax, of the depreciated gross profit. Figure D5-1 shows the annual, discrete cash flow

over 20 years of operation..

Table D5-4

Conservative Case Scenario Net Profit Calculations

Year	0	1-10	11-20
Capital Investment	-$48,338,996	$0	$0
Revenue	$0	$816,000,000	$816,000,000
COGS	$0	-$193,386,423	-$193,386,423
Gross Profit	**-$48,338,996**	**$622,613,577**	**$622,613,577**
Depreciation	$0	-$4,833,900	$0
Taxes	$0	-$185,333,903	-$186,784,073
Net Cash Flow	**-$48,338,996**	**$432,445,774**	**$435,829,504**
Net Profit	**-$48,338,996**	**$437,279,674**	**$435,829,504**

Figure D5-1

Discrete Cash Flow for Conservative Case Scenario
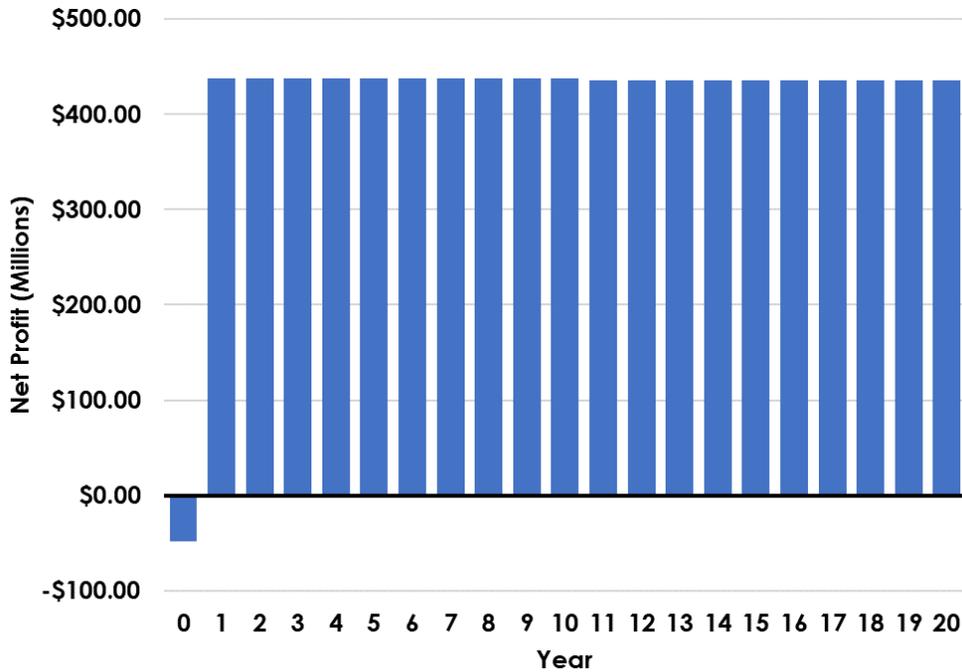
We conducted a discounted cash flow analysis to find the profitability of the plant over 20 years of production. Subsequently, we calculated the return on investment (ROI), internal rate of return (IRR), and net present value (NPV). Assuming the discount rate is 11% (i), we calculated the discounted cash flow using Equation D5-1, with t being the year of operation. We calculated the ROI (Equation D5-2) by dividing the NPV by the initial invested capital (C_i). Finally, we solved for the IRR by setting NPV to 0 (Equation D5-3), where C_t is the annual cash flow for year t (Towler & Sinnott, 2012). The cumulative discounted cash flow over 20 years is summarized in Table D5-5 and Figure D5-2.

$$\text{Equation D5-1. } Discounted\ Cash\ Flow = \frac{Annual\ Cash\ Flow}{(1+i)^t}$$

$$\text{Equation D5-2. } ROI = \frac{NPV}{C_i}$$

$$\text{Equation D5-3. } NPV = 0 = \Sigma_{t=1}^{T} \frac{C_t}{(1+IRR)^t} - C_i$$

Table D5-5

Conservative Case Scenario Discounted Cash Flow Calculations

Year	Cash Flow	Discounted Cash Flow	Cumulative Discounted Cash Flow
0	-$48,338,996	-$48,338,996	-$48,338,996
1	$437,279,674	$393,945,652	$345,606,656
2	$437,279,674	$354,905,993	$700,512,649
3	$437,279,674	$319,735,129	$1,020,247,778
4	$437,279,674	$288,049,666	$1,308,297,443
5	$437,279,674	$259,504,203	$1,567,801,646
6	$437,279,674	$233,787,570	$1,801,589,217
7	$437,279,674	$210,619,433	$2,012,208,650
8	$437,279,674	$189,747,237	$2,201,955,887
9	$437,279,674	$170,943,457	$2,372,899,343
10	$437,279,674	$154,003,114	$2,526,902,457
11	$435,829,504	$138,281,429	$2,665,183,887
12	$435,829,504	$124,577,864	$2,789,761,751
13	$435,829,504	$112,232,310	$2,901,994,061
14	$435,829,504	$101,110,189	$3,003,104,251
15	$435,829,504	$91,090,261	$3,094,194,512
16	$435,829,504	$82,063,298	$3,176,257,810
17	$435,829,504	$73,930,899	$3,250,188,709
18	$435,829,504	$66,604,414	$3,316,793,122
19	$435,829,504	$60,003,976	$3,376,797,098
20	$435,829,504	$54,057,636	**$3,430,854,735**

Figure D5-2

Cumulative Discounted Cash Flow for Conservative Case Scenario
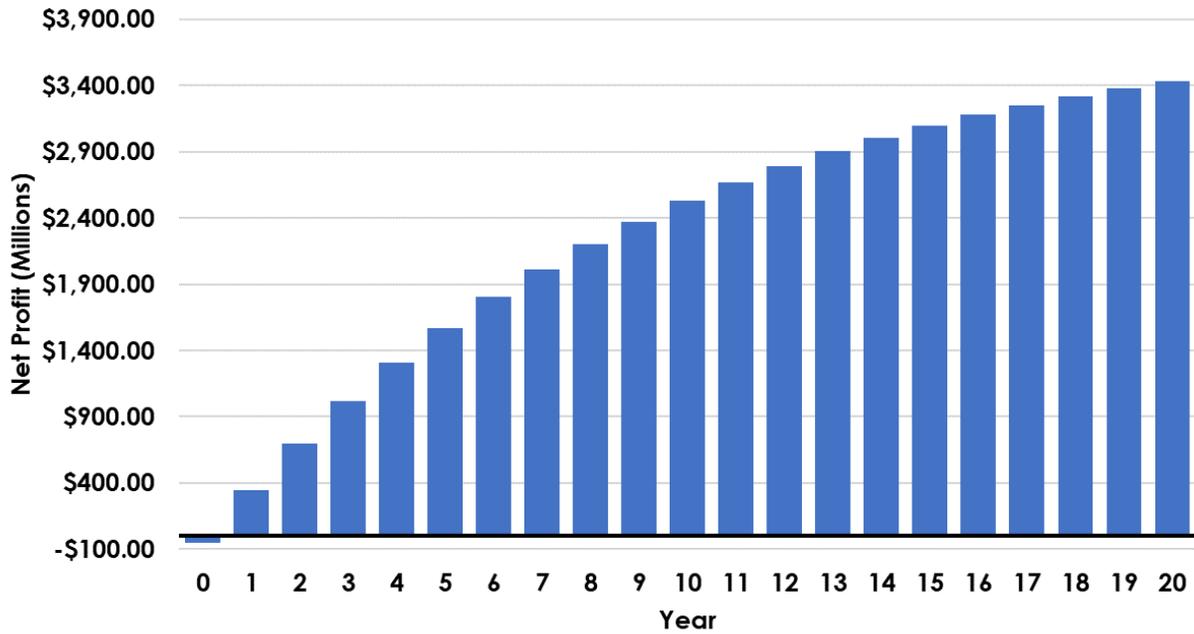
Table D5-6

Conservative Case Scenario ROI, IRR, and NPV after 20 Years

ROI	IRR	NPV
7097.49%	904.61%	$3,430,854,735

In this conservative scenario where only the expected demand quantity of vaccines would be sold, the values of ROI, IRR, and NPV after 20 years (Table D5-6) are large. Thus, the plant will be profitable due to a relatively small capital investment and a substantial annual net profit.

5.3.2 Scenario 2: Best Case

In our calculation for expected demand, we did not account for all newborns and children under five years of age in SSA. In addition, we did not account for the potential market of

vaccinating children older than five years of age and adults. As a result, it is possible that demand is greater than we initially expected. In a best case scenario, we will be able to sell all of our surplus vaccines with a revenue of $849,300,000. Assuming similar trends in depreciation and taxes as in the conservative case scenario, we modeled the discrete (Figure D5-3) and cumulative discounted cash flow (Figure D5-4) for this scenario.

Figure D5-3

Discrete Cash Flow for Best Case Scenario
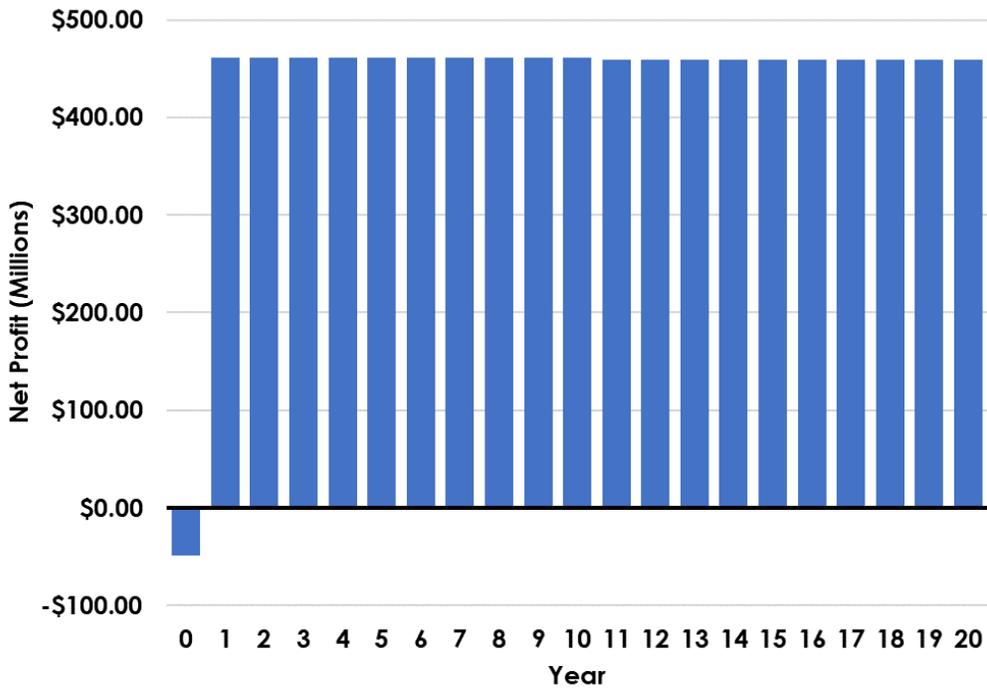
Figure D5-4

Cumulative Discounted Cash Flow for Best Case Scenario
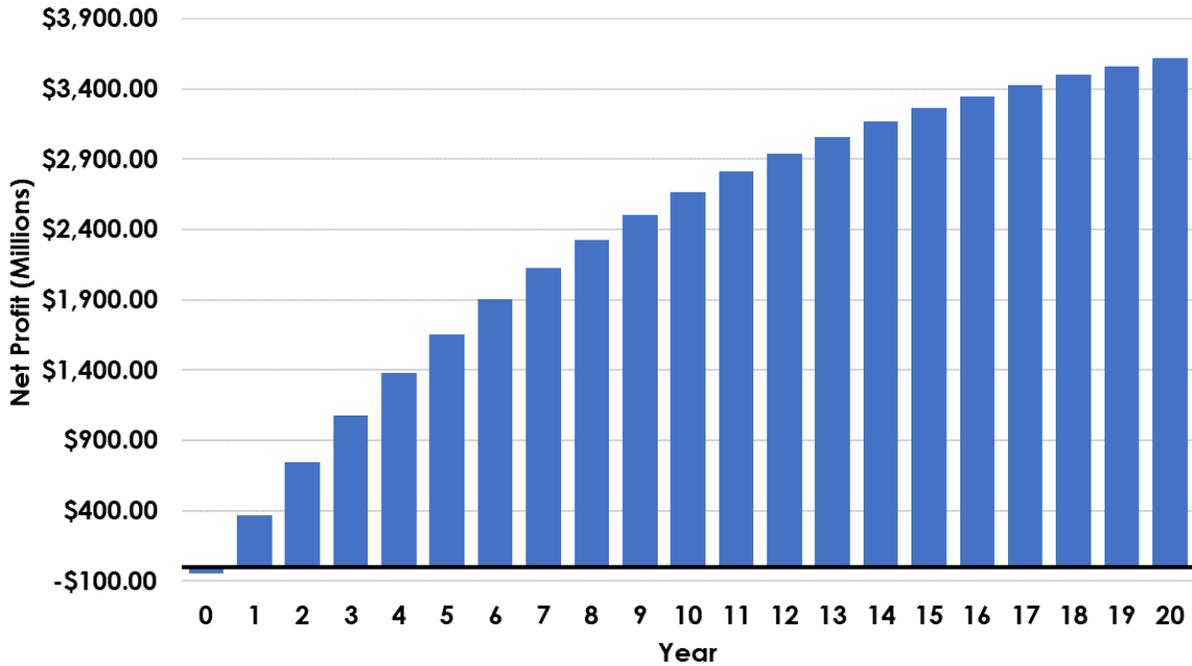
Table D5-7

Best Case Scenario ROI, IRR, and NPV after 20 Years

ROI	IRR	NPV
7481.52%	952.84%	$3,616,491,201

In the best case scenario where all vaccines would be sold, the values of ROI, IRR, and NPV after 20 years (Table D5-7) are large. Thus, under the best case scenario, the plant will be extremely profitable.

5.3.3 Scenario 3: 50% Market Penetration

In SSA, childhood vaccination rates in general are low, in part due to insufficient infrastructure and vaccine hesitancy. As a result, it is possible that we do not sell all of our

produced vaccines. Assuming that we are only able to sell 50% of the expected vaccine demand, this would significantly affect the profitability of the plant. In this scenario, after one year of operation at this 50% market penetration level, we immediately react by reducing operating costs by 50% in order to increase gross profit. This would entail producing half as many batches as we initially intended, and would involve running half as many batches. Assuming similar trends in depreciation and taxes as in the conservative case scenario, we modeled the discrete (Figure D5-5) and cumulative discounted cash flow (Figure D5-6) for this scenario.

Figure D5-5

Discrete Cash Flow for 50% Market Penetration Scenario
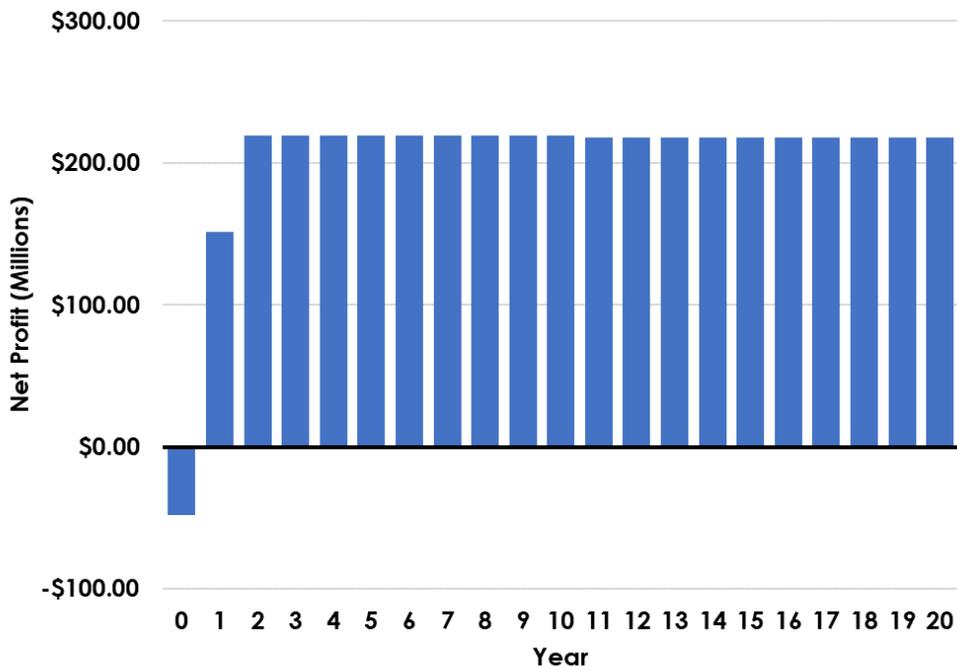
Figure D5-6

Cumulative Discounted Cash Flow for 50% Market Penetration Scenario
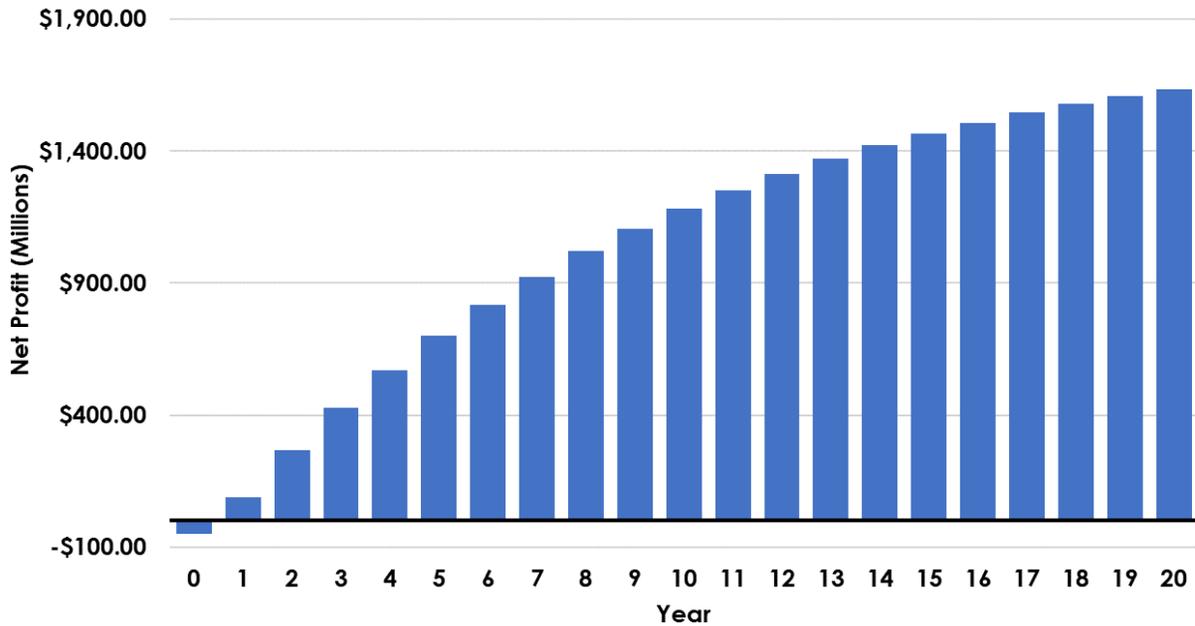
Table D5-8

50% Market Penetration Scenario ROI, IRR, and NPV after 20 Years

ROI	IRR	NPV
3381.43%	345.23%	$1,634,550,362

In this scenario, we expect to have high ROIs, IRR, and NPVs after 20 years of operation (Table D5-8). We also expect to recoup all of our capital investment within the first year of operation. Thus, under these poor operating conditions, our proposed plant design will be profitable due to the sizable revenue generated when compared to the initial capital investment.

5.3.4 Scenario 4: Market Competition

Current research into malaria has spawned the development and testing of a variety of vaccine candidates. One such candidate, the *P. falciparum* CSP mRNA-LNP1 vaccine, demonstrates 88% efficacy in mice (Mallory et al., 2021). As a result, this vaccine poses serious competition with our product. Since the mRNA vaccine is within early stages of clinical trial testing, we expect the vaccine to only reach market approximately five years after we start production, assuming an accelerated timeline for vaccine approval. After the new vaccine is produced and distributed, we estimated a 75% reduction in our conservative estimate for sales as a worst case scenario. Immediately after seeing reduced plant profitability for one year, we will cut our operating costs by 75%. Assuming similar trends in depreciation and taxes as in the conservative case scenario, we modeled the discrete (Figure D5-7) and cumulative discounted cash flow (Figure D5-8) for this scenario.

As with the previous two scenarios, we expect to have high ROIs, IRR, and NPVs after 20 years of operation (Table D5-9). We again expect to recoup all of our capital investment within the first year of operation. Thus, under these non-ideal operating conditions, our proposed plant design will remain profitable.

Figure D5-7

Discrete Cash Flow for Market Competition Scenario
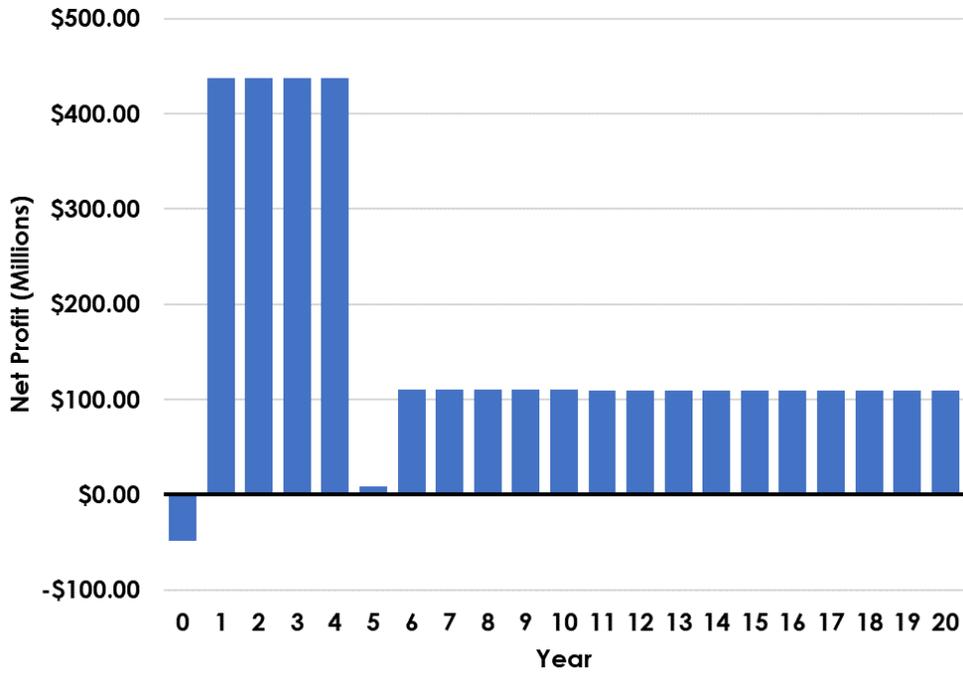
Figure D5-8

Cumulative Discounted Cash Flow for Market Competition Scenario
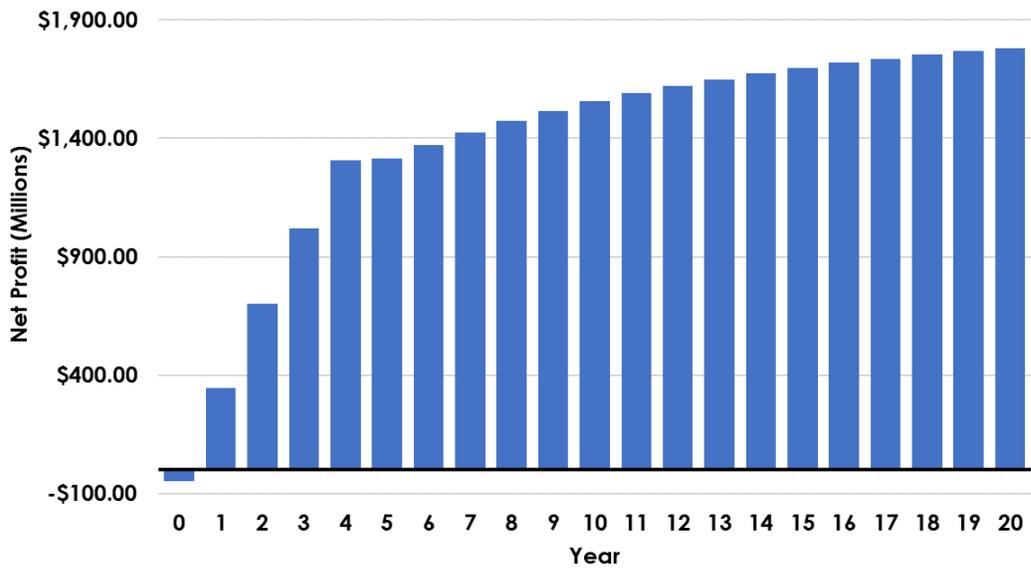
Table D5-9

Market Competition Scenario ROI, IRR, and NPV after 20 Years

ROI	IRR	NPV
3685.88%	904.53%	$1,781,715,901

6. Safety, Environmental, & Social Considerations

6.1 Safety and Sterility

Safety during pharmaceutical manufacturing involves safe laboratory practices and safe industrial practices. There are inherent dangers associated with using methanol as a carbon source for a bioreactor in commercial production due to its highly flammable and toxic properties. Long-term exposure to methanol can result in blindness, organ failure, and even death because the vapors are so easily ignited and can start fires or explode. Therefore, when working with methanol in a bioreactor, it is crucial to adhere to strict safety procedures. Through the use of proper personal protective equipment (PPE), the risks to employees and the product may be minimized. Additionally, in the pharmaceutical industry, sterility requirements for injectables are more stringent as the final product is administered to people. To better ensure sterility, more barriers are used to prevent contaminants from entering the product. The use of HEPA filters, airlocks, air pressure gradients, microbial plate readers, and additional PPE (eg. face masks and gowns) are ways to ensure sterility. In addition, because equipment can present hazards during the process (eg. high pressure, high temperature, and rotating parts), all operators will be thoroughly trained and required to wear proper safety PPE before they are given independent tasks.

To ensure that the final product meets WHO and SAHPRA purity specifications, a Quality Assurance (QA) team will test product purity throughout the process. Most steps have a

range of acceptable purities, since the final product will pass through a sterile filter. However, if a product fails to meet the specifications anytime throughout the process, then the batch will be discarded. In this case, the additional time after our estimated plant operational time may be used to run additional batches. Regardless, according to our economic analyses, the loss of a batch will not harm plant profitability significantly.

6.2 Environmental Impact

Under the Resource Conservation and Recovery Act, any material in contact with pharmaceutical products should be treated as hazardous waste. Release of biological products like vaccines may have unintended consequences on nearby ecosystems (National Institute of Health, 2020). Environmental cost across the life cycle of this process includes impacts of raw material production, transportation, energy and waste. We will focus on the environmental impact of the waste leaving the facility.

6.2.1 Upstream

The shake flasks will use detergent for cleaning after use. These cleaning solutions must be disposed of appropriately as industrial chemical waste as detergents are some of the primary chemical pollutants that affect aquatic ecosystems (Giagnorio et al., 2017). The 2.5 L, 50 L, and production scale bioreactors each utilize a single-use plastic fermentation bag. Each single-use plastic bag must be thoroughly decontaminated and then subsequently sent to a waste incineration facility. The cost of plastic disposal will be directly correlated with the distance necessary to transport the plastic waste as well as the volume of plastic waste requiring disposal. Incineration is a quality method of plastic disposal as it reduces waste quantity as well as pollution when compared to landfills. However, depositing our potentially contaminated plastics

into landfills may inadvertently lead to chemical contamination in the surrounding environment. There is a risk that incineration may release pollutants into the atmosphere, but this is largely regulated via the use of filters.

Aside from waste generated via cleaning, carbon dioxide will be the main waste compound being expelled from the bioreactors during operation. However, given the relatively small quantity of our product, the small amount of generated carbon dioxide gas may be safely vented.

6.2.2 Downstream

Because our process utilizes some single-use equipment, we must consider the safe disposal of those materials. Cytiva's ReadyToProcess Columns (including the Capto Core 700 column used in this process) should not be deconstructed before disposal. Our process, which uses one disposable Capto Core 700 each year, will decontaminate columns before sending them to hazardous waste disposal facilities.

Most waste streams will be sent to a waste disposal center due to toxicity, accumulation in the environment or in organisms, or directly touching the vaccine product. Not all components in each stream are dangerous to the environment, but the presence of any dangerous component in a waste stream signifies that the stream must be disposed of as industrial chemical waste. Because most of the waste streams are neutral, they will not require pretreatment before disposal.

In high-pressure homogenization, the cell slurry from the centrifugation step prior is suspended in PLB. PLB, comprising Triton, EDTA, $MgCl_2$ and Tris may have negative impacts on both terrestrial plants and aquatic life. Trees in particular are susceptible to chloride poisoning from the dissolved salt (*Environmental Impacts of Road Salt and Other De-Icing Chemicals*,

n.d.). As chloride accumulates in leaves, they turn yellow and die. Dissolved $MgCl_2$ salt has a

proclivity to travel through groundwater. In waterways, $MgCl_2$ contributes to softening water.

Higher magnesium levels in water are associated with an increase in heavy metal toxicity. EDTA

is slow to degrade in the environment but is minimally toxic to terrestrial plants and animals.

Algae and invertebrates are most susceptible to EDTA toxicity, living primarily in water. EDTA

is soluble and travels easily through groundwater without being sorbed by soil (Environmental

Protection Agency, 2004). Tris has no ecotoxicity concerns (Thermo Fisher Scientific, 2020a).

Triton is considered to be hazardous towards aquatic life and has been determined to be slightly

toxic to rats on the Hodge and Sterner scale (Canadiation Centre for Occupational Health and

Safety, n.d.; Thermo Fisher Scientific, 2020b). Triton does not contain any hazardous air

pollutants.

The Capto Core 700, which itself will be disposed of every year, requires a series of

buffers, including an initial equilibration step with more PLB. After equilibration, the sample

suspended in the same buffer is passed through. Sodium hydroxide is introduced to the column

for SIP. This 1 M sodium hydroxide solution and 30% isopropanol (IPA) will have a pH ~13 and

so it must be neutralized before being disposed of. NaOH has no impact on air quality because

of its low vapor pressure (Arkema, 2013). Any aerosolized NaOH is neutralized by CO_2 in the

air. As NaOH travels through the ground, some may be neutralized in the pores of soil. However,

because of NaOH's high solubility in water, it can travel easily travel through the ground

dissolved in water and may pose a risk to aquatic life if pH is affected dramatically by large

volumes of NaOH. IPA is practically nontoxic in rats on the Hodge and Sterner scale (National

Research Council US Committee on Toxicology, 1984). Only in very high concentrations will it

be toxic to aquatic life so the risk is low. IPA degrades readily in the environment and will not accumulate in organisms (LyondellBasell, 2015).

However, the citric acid stream from affinity chromatography can be mixed with the basic sodium hydroxide CIP/SIP streams for neutralization. The stoichiometric ratio of citric acid to sodium hydroxide is 3:1 and there is twice as much NaOH used in the process than citric acid. The surplus of NaOH waste streams must be neutralized. This will form a sodium citrate solution which can be flushed to the sewer in compliance with National Institute of Health guidelines (National Institute of Health, 2020). The remaining volume of NaOH and IPA solution will be sent to a hazardous waste facility. Sodium citrate has high solubility in water so it can travel easily through the environment. However, microorganisms will quickly degrade it in the environment. Sodium citrate has a low toxicity in aquatic life and is considered slightly toxic in rats on the Hodge and Sterner scale (United States Department of Agriculture, 2017).

The citric acid for sanitizing the affinity chromatography is considered practically non-toxic on the Hodge and Sterner scale in rats, but has higher toxicity in aquatic life (*Citric Acid SIDS Initial Assessment Report*, 2000). There is no risk to air quality. Citric acid biodegrades readily in the environment and does not accumulate within organisms. All of the citric acid will be mixed with NaOH so there will be no excess leaving the facility.

6.2.3 Formulation & Fill-Finish

Aside from sterile filtration waste and the carbon emissions produced via heavy electricity utilization in the Formulation & Fill-Finish stage of vaccine production, there is little waste produced as a direct result of the process. However, the final product is packaged in vials and administered via syringes, both of which produce a considerable amount of medical waste.

In addition, discarded vials containing preservatives may poison marine life and medical waste incineration produces gas with high concentrations of dioxins. Moreover, there will be a massive increase in greenhouse gas emissions as a result of distribution and storage of the vaccines. Protective equipment for immunization campaigns also contributes towards the waste and often shows up in water systems as microplastics (Hasija et al., 2022). However, since the majority of this waste is produced after the vaccine product has been packaged, directly dealing with this waste is outside of the scope of our design and considerations. We will have to work with governments of SSA to ensure that proper protocols for the disposal of medical waste are followed.

6.3 Social Impact

By placing our production facility in South Africa, we minimize the transportation distance and time for distributing the vaccines to consumers in SSA. This helps to limit the burden of vaccine distribution on Africa's infrastructure. Moreover, since Africa's infrastructure is not developed well enough to maintain long-term R21c stability at the low-temperature specifications (-80℃), thus limiting the product shelf life, the decrease in transportation time associated with locating the manufacturing facility on the continent will be advantageous. In addition to minimizing transportation, the location facilitates Africa to depend less on other parts of the world for vaccination supplies. Currently, Africa is not self-sufficient in vaccine production: 99% of administered COVID-19 vaccines were manufactured outside of the continent (Erondu, 2022). The addition of another vaccine manufacturing facility, via our proposed manufacturing plant, on the continent will help improve Africa's biopharmaceutical infrastructure. For instance, the plant will support the hiring of six supervisors and 30 operators, generating at least 36 new jobs for South Africans. This infrastructure improvement will enable

the country to move towards becoming less reliant on foreign medical products. The decrease in reliance will likely help increase vaccine acceptance among Africans, some of whom distrust Western medicine due to its association with Western colonization of Africa (Chutel & Fisher, 2021).

Other social issues, aside from those relating to plant location, include vaccine pricing. To make the vaccines affordable to SSA governments, we chose to sell our vaccine products at $3/dose, the ceiling price of COVID-19 vaccines delivered to low and middle-income countries (Gavi Staff, 2020). Partnerships with Gavi and the Gates Foundation for distribution will potentially help us decrease the effective vaccine price to the consumer, preventing cost from being a barrier to vaccine uptake.

Although we expect the R21c/Matrix-M vaccine to be safe and to have a high efficacy in preventing malaria infections, the drug is still undergoing Phase II and III clinical trial testing. As a result, the vaccines are not yet approved for use and it is possible that in future research, issues with vaccine safety become apparent. In recently published clinical trial data, reported serious adverse events in participants appeared to be unrelated to the vaccine. Thus, in the absence of additional data, we will assume that there are minimal adverse side effects to R21c/Matrix-M vaccine injections and that the vaccine is on track for approval in the near future.

E. Conclusions and Recommendations

Our technical design for the R21c/Matrix-M vaccine plant allows for the production of 1.42 kg of R21c, or 283,100,680 single-dose vaccines, to vaccinate 68 million children and newborns each year. This production capacity exceeds the initial goal of producing 1.36 kg of R21c in 272 million single-dose vaccines per year. In our designed process, our major equipment include a production-scale bioreactor, Capto Core 700 column, C-tag Affinity Chromatography

column, and vial filling and lyophilization apparatuses. Interspersed between these equipment, we include a variety of filtration steps to help further purify our final product. The overall recovery and yield of R21c VLPS throughout our designed purification processes is 43%. Our final vaccine will be distributed from the plant's location in South Africa to the target SSA countries. Prior to vaccine administration, the R21c vaccines will be reconstituted with Matrix-M solution.

Our economic analysis of this proposed design suggests that our project will be profitable. After 20 years of operation after the initial plant setup, a conservative estimate of the IRR is 905.7% and NPV is $3,435,000,000, yielding an ROI of 7097%. Under our conservative case scenarios, and even the 50% market penetration and market competition scenarios, our process has an impressive return on investment. Therefore, we recommend that further research and pilot plant development move forward to determine whether or not this project is feasible considering more exact design data.

There are a variety of potential areas of improvement and exploration for future plant design analysis. For instance, we are currently running at a high production surplus of vaccines, which we would ideally like to minimize. Further analysis into batch and upstream design will be desirable to make the process more economically favorable. We also recommend that more research be done into other target populations, such as adults and people outside of SSA, to whom we may sell our surplus vaccines, thus increasing our revenue and profit. Minimizing medical waste, and the purchase of packaging, by producing multi-dose instead of single-dose vials, may also contribute to a higher profit, in addition to minimizing the plant's impact on the environment.

In terms of the purification process design, we recommend investigating major design changes. Currently, the Serum Institute is producing R21, which no longer contains the C-tag, in *Hansenula polymorpha* for phase II and III of clinical trials (Datoo et al., 2021). We suggest looking into how to maintain purity standards without the addition of the C-tag, as well as into the protein production performance of *H. polymorpha* in comparison to *P. pastoris*. We also recommend investigating the use of another host cell that can grow and express the R21c protein without methanol as the carbon source to avoid the safety concerns of using methanol in a commercial bioreactor design. Other design considerations include using more exact experimental data for designing the chromatography steps, as well as constructing the production bioreactors to be shorter and to use less power.

Despite the potential for improvement, we expect that building and operating the proposed R21c vaccine manufacturing facility will be a profitable endeavor. Located in South Africa, with close ties to the local Biovac facility, our plant will also be able to minimize distribution costs due to the close proximity to SSA. Moreover, the African-based plant will encourage vaccine acceptance from those wary of western-made medical products and help grow South African infrastructure. However, understanding that SSA infrastructure may not be able to support the cold storage required for vaccine distribution, future research should analyze how to manufacture the vaccine to be stable at higher temperatures and to develop distribution protocols that work within the limits of SSA infrastructure. Regardless, we believe that this plant will tremendously help SSA deal with the burden of malaria, and we should move forward to the next phase of plant design and implementation.

F. Acknowledgements

G. References

AKTA Ready XL. (n.d.). Cytiva.

https://www.cytivalifesciences.com/en/us/shop/chromatography/chromatography-systems

/akta-ready-xl-p-09645#:~:text=%C3%84KTA%20ready%20XL%20provides%20high,in

%20large%2Dvolume%20bioreactor%20cultures.

AlfaLaval BTUX 305. (2018).

https://www.alfalaval.com/globalassets/documents/products/separation/centrifugal-separa

tors/disc-stack-separators/btux-305_pchs00094en.pdf?_ga=2.36004640.124862937.1676

944202-1759049358.1676944202&_gl=1*18bxbs8*_ga*MTc1OTA0OTM1OC4xNjc2O

TQ0MjAy*_ga_VR90J5D3K9*MTY3Njk0NDIwMi4xLjEuMTY3Njk0NjQ5Ny4wLjAu

MA..

Ariete NS3037. (2010).

https://www.gea.com/en/binaries/ariete-NS3037-high-pressure-homogenizer-pump-datas

heet_tcm11-38670.pdf

Arkema. (2013). *Sodium Hydroxide GPS Safety Summary*.

https://www.arkema.com/files/live/sites/shared_arkema/files/downloads/socialresponsabil

ity/safety-summuries/hydrogen-peroxide-naoh-sodium-hydroxide-gps-2013-02-10-v0.pdf

Canadiation Centre for Occupational Health and Safety. (n.d.). *What is a LD50 and LC50?*

CCOHS. https://www.ccohs.ca/oshanswers/chemicals/ld50.html

Canales, C., Altamirano, C., & Berrios, J. (2018). The growth of Pichia pastoris Mut+ on

methanol–glycerol mixtures fits to interactive dual-limited kinetics: Model development

and application to optimised fed-batch operation for heterologous protein production.

Bioprocess and Biosystems Engineering, *41*(12), 1827–1838.

https://doi.org/10.1007/s00449-018-2005-1

Capto Core 700. (n.d.). MilliporeSigma. Retrieved November 7, 2022, from

https://www.sigmaaldrich.com/US/en/technical-documents/technical-article/protein-biolo

gy/protein-purification/capto-core-700

Carta, G. (2021). *Heat and Mass Transfer for Chemical Engineers: Principles and Applications*

(1st edition). McGraw Hill.

Çelik, E., Çalık, P., & Oliver, S. G. (2009). A structured kinetic model for recombinant protein

production by Mut+ strain of Pichia pastoris. *Chemical Engineering Science*, *64*(23),

5028–5035. https://doi.org/10.1016/j.ces.2009.08.009

Cervera, L., Gòdia, F., Tarrés-Freixas, F., Aguilar-Gurrieri, C., Carrillo, J., Blanco, J., &

Gutiérrez-Granados, S. (2019). Production of HIV-1-based virus-like particles for

vaccination: Achievements and limits. *Applied Microbiology and Biotechnology*,

103(18), 7367–7384. https://doi.org/10.1007/s00253-019-10038-3

Chutel, L., & Fisher, M. (2021, December 1). The Next Challenge to Vaccinating Africa:

Overcoming Skepticism. *The New York Times*.

https://www.nytimes.com/2021/12/01/world/africa/coranavirus-vaccine-hesitancy-africa.

html

Citric Acid SIDS Initial Assessment Report. (2000).

Cleaning Laboratory Glassware. (n.d.). MilliporeSigma. Retrieved April 4, 2023, from

https://www.sigmaaldrich.com/US/en/technical-documents/protocol/chemistry-and-synth

esis/reaction-design-and-optimization/cleaning-glassware#Dishes-and-Culture-Bottles

Collins, K. A. (2014). *R21, a novel particle based vaccine for a multi-component approach to*

malaria vaccination. St Cross College, University of Oxford.

Collins, K. A., Snaith, R., Cottingham, M. G., Gilbert, S. C., & Hill, A. V. S. (2017). Enhancing

protective immunity to malaria with a highly immunogenic virus-like particle vaccine.

Scientific Reports, *7*(1), Article 1. https://doi.org/10.1038/srep46621

Collins, K., Brod, F., Snaith, R., Ulaszewska, M., Longley, R., Salman, A., Gilbert, S., Spencer,

A., Franco, D., Ballou, W., & Hill, A. (2021). Ultra-low dose immunization and

multi-component vaccination strategies enhance protection against malaria in mice.

Scientific Reports, *11*, 10792. https://doi.org/10.1038/s41598-021-90290-8

Cowman, A. F., Healer, J., Marapana, D., & Marsh, K. (2016). Malaria: Biology and Disease.

Cell, *167*(3), 610–624. https://doi.org/10.1016/j.cell.2016.07.055

Cregg, J. M., Cereghino, J. L., Shi, J., & Higgins, D. R. (2000). Recombinant Protein Expression

in Pichia pastoris. *Molecular Biotechnology*, *16*(1), 23–52.

https://doi.org/10.1385/MB:16:1:23

Cytiva. (n.d.). *Chromaflow chromtography columns*. Cytiva Life Sciences.

https://www.cytivalifesciences.com/en/us/shop/chromatography/columns/process-column

s/chromaflow-chromatography-columns-p-06319

Cytiva. (2018). *Evaluation of performance of a disposable mAb affinity chromatography

column used over multiple process cycles*.

https://cdn.cytivalifesciences.com/api/public/content/digi-24020-pdf

Cytiva. (2020a). *ReadyToProcess columns User Manual*.

https://cdn.cytivalifesciences.com/api/public/content/digi-26620-pdf

Cytiva. (2020b). *Capto Core 400 Capto Core 700 Multimodal Chromatography*.

https://cdn.cytivalifesciences.com/api/public/content/digi-16188-pdf#:~:text=Capto%E2

%84%A2%20Core%20400%20and,viruses%20and%20other%20large%20biomolecules.

Cytiva. (2022). *SA25 Aseptic Filling Workcell*.

Cytiva. (2023). *ReadyToProcess Capto Core 700*. Cytiva.

    https://www.cytivalifesciences.com/en/us/shop/chromatography/prepacked-columns/mult

    imodal/readytoprocess-capto-core-700-p-09582

Czyż, M., & Pniewski, T. (2016). Thermostability of Freeze‑Dried Plant‑Made VLP‑Based

    Vaccines. In J. del R. Olvera (Ed.), *Sustainable Drying Technologies*. IntechOpen.

    https://doi.org/10.5772/63503

Datoo, M. S., Natama, H. M., Somé, A., Bellamy, D., Traoré, O., Rouamba, T., Tahita, M. C.,

    Ido, N. F. A., Yameogo, P., Valia, D., Millogo, A., Ouedraogo, F., Soma, R., Sawadogo,

    S., Sorgho, F., Derra, K., Rouamba, E., Ramos-Lopez, F., Cairns, M., … Tinto, H. (2022).

    Efficacy and immunogenicity of R21/Matrix-M vaccine against clinical malaria after 2

    years' follow-up in children in Burkina Faso: A phase 1/2b randomised controlled trial.

    The Lancet Infectious Diseases. https://doi.org/10.1016/S1473-3099(22)00442-X

Datoo, M. S., Natama, M. H., Somé, A., Traoré, O., Rouamba, T., Bellamy, D., Yameogo, P.,

    Valia, D., Tegneri, M., Ouedraogo, F., Soma, R., Sawadogo, S., Sorgho, F., Derra, K.,

    Rouamba, E., Orindi, B., Ramos Lopez, F., Flaxman, A., Cappuccini, F., … Tinto, H.

    (2021). Efficacy of a low-dose candidate malaria vaccine, R21 in adjuvant Matrix-M,

    with seasonal administration to children in Burkina Faso: A randomised controlled trial.

    The Lancet, *397*(10287), 1809–1818. https://doi.org/10.1016/S0140-6736(21)00943-0

D'Souza, J., & Nderitu, D. (2021). Ethical considerations for introducing RTS,S/AS01 in

    countries with moderate to high Plasmodium falciparum malaria transmission. *The*

    Lancet Global Health, *9*(12), e1642–e1643.

    https://doi.org/10.1016/S2214-109X(21)00498-8

Environmental impacts of road salt and other de-icing chemicals. (n.d.). Minnesota Stormwater

    Manual.

    https://stormwater.pca.state.mn.us/index.php/Environmental_impacts_of_road_salt_and_

    other_de-icing_chemicals

Environmental Protection Agency. (2004). *Tolerance Reassessment Decisions Completed by the*

    Lower Toxicity Pesticide Chemical Focus Group.

    https://www.epa.gov/sites/default/files/2015-04/documents/edta.pdf

Erondu, N. (2022, August 3). *Now is the moment to launch an African vaccine industry*.

    Chatham House.

    https://www.chathamhouse.org/publications/the-world-today/2022-08/now-moment-laun

    ch-african-vaccine-industry

ExPASy—ProtParam tool. (n.d.). Retrieved November 7, 2022, from

    https://web.expasy.org/protparam/

Filter-Loop-Assembly. (2016). Sartorius.

    https://www.sartorius.com/shop/ww/en/usd/bioprocess-products-%26-services-filtration-a

    nd-purification-technologies-virus-filtration-uv-c-inactivation/filter-loop-assembly/p/4X

    C39

Gavi Staff. (2020, September 29). *New collaboration makes further 100 million doses of*

    COVID-19 vaccine available to low- and middle-income countries | Gavi, the Vaccine

    Alliance.

    https://www.gavi.org/news/media-room/new-collaboration-makes-further-100-million-do

    ses-covid-19-vaccine-available-low

Giagnorio, M., Amelio, A., Gruttner, H., & Tiraferri, A. (2017). Environmental impacts of

detergents and benefits of their recovery in the laundering industry. *Journal of Cleaner*

    Production, *Volume 154*. https://doi.org/10.1016/j.jclepro.2017.04.012

Gil Dhawan. (1985, July). *Back to Basics: About Ultrafiltration (UF)*.

    https://www.appliedmembranes.com/back-to-basics-about-ultrafiltration-uf.html

Global Pumps. (n.d.). *List of Typical Viscosities*. Retrieved March 2, 2023, from

    https://www.globalpumps.com.au/list-of-typical-viscosities

Green, D., & Southard, M. (2019). *Perry's Chemical Engineers' Handbook, 9th Edition.*

    McGraw-Hill Education: New York, Chicago, San Francisco, Athens, London, Madrid,

    Mexico City, Milan, New Delhi, Singapore, Sydney, Toronto.

Hasija, V., Patial, S., Kumar, A., Singh, P., Ahamad, T., Khan, A. A. P., Raizada, P., & Hussain,

    C. M. (2022). Environmental impact of COVID-19 Vaccine waste: A perspective on

    potential role of natural and biodegradable materials. *Journal of Environmental Chemical*

    Engineering, *10*(4), 107894. https://doi.org/10.1016/j.jece.2022.107894

Invitrogen. (2002). *Pichia Fermentation Process Guidelines*.

    https://tools.thermofisher.com/content/sfs/manuals/pichiaferm_prot.pdf

Jin, J., Hjerrild, K., Silk, S., Brown, R., Labbé, G., Marshall, J., Wright, K., Bezemer, S.,

    Clemmensen, S., Biswas, S., Li, Y., El-Turabi, A., Douglas, A., Hermans, P., Detmers, F.,

    de Jongh, W., Higgins, M., Ashfield, R., & Draper, S. (2017). Accelerating the clinical

    development of protein-based vaccines for malaria by efficient purification using a four

    amino acid C-terminal 'C-tag.' *International Journal for Parasitology*, *47*.

    https://doi.org/10.1016/j.ijpara.2016.12.001

Joi, P. (2023). *Five things you need to know about the new R21 malaria vaccine*. Gavi.

    https://www.gavi.org/vaccineswork/five-things-you-need-know-about-new-r21-malaria-v

accine

Jordà, J., Jouhten, P., Cámara, E., Maaheimo, H., Albiol, J., & Ferrer, P. (2012). Metabolic flux

profiling of recombinant protein secreting Pichia pastoris growing on glucose:methanol

mixtures. *Microbial Cell Factories*, *11*(1), 57. https://doi.org/10.1186/1475-2859-11-57

Lagoutte, P., Mignon, C., Donnat, S., Stadthagen, G., Mast, J., Sodoyer, R., Lugari, A., & Werle,

B. (2016). Scalable chromatography-based purification of virus-like particle carrier for

epitope based influenza A vaccine produced in Escherichia coli. *Journal of Virological*

Methods, *232*, 8–11. https://doi.org/10.1016/j.jviromet.2016.02.011

Ledford, H. (2022). Malaria vaccine booster prolongs protection. *Nature*.

https://doi.org/10.1038/d41586-022-02902-6

Li, P., Anumanthan, A., Gao, X.-G., Ilangovan, K., Suzara, V. V., Düzgüneş, N., &

Renugopalakrishnan, V. (2007). Expression of Recombinant Proteins in Pichia Pastoris.

Applied Biochemistry and Biotechnology, *142*(2), 105–124.

https://doi.org/10.1007/s12010-007-0003-x

Liang, J., & Yuan, J. (2007). Oxygen transfer model in recombinant Pichia pastoris and its

application in biomass estimation. *Biotechnology Letters*, *29*(1), 27–35.

https://doi.org/10.1007/s10529-006-9203-7

LyondellBasell. (2015). *Global Product Strategy Safety Summary: Isopropyl Alcohol*. Global

Product Strategy (GPS) Safety Summary

MabCaptureC Protein A Chromatography Resin. (n.d.). Thermo Fisher Scientific.

Malairuang, K., Krajang, M., Sukna, J., Rattanapradit, K., & Chamsart, S. (2020). High Cell

Density Cultivation of Saccharomyces cerevisiae with Intensive Multiple Sequential

Batches Together with a Novel Technique of Fed-Batch at Cell Level (FBC). *Processes*,

8(10), Article 10. https://doi.org/10.3390/pr8101321

Mallory, K. L., Taylor, J. A., Zou, X., Waghela, I. N., Schneider, C. G., Sibilo, M. Q., Punde, N.
M., Perazzo, L. C., Savransky, T., Sedegah, M., Dutta, S., Janse, C. J., Pardi, N., Lin, P. J.
C., Tam, Y. K., Weissman, D., & Angov, E. (2021). Messenger RNA expressing PfCSP
induces functional, protective immune responses against malaria in mice. *Npj Vaccines*,
6(1), Article 1. https://doi.org/10.1038/s41541-021-00345-0

Mandavilli, A., & Cheng, K.-C. (2022, October 4). At Long Last, Can Malaria Be Eradicated?
The New York Times. https://www.nytimes.com/2022/10/04/health/malaria-vaccines.html

Masterflex Peristaltic Pumps and Fluid Handling Solutions. (2023). Avantor.
https://us.vwr.com/cms/masterflex-fluid-handling-solutions

Mi, X., Fuks, P., Wang, S.-C., Winters, M. A., & Carta, G. (2021). Protein Adsorption on
Core-shell Particles: Comparison of Capto™ Core 400 and 700 Resins. *Journal of
Chromatography. A*, *1651*, 462314. https://doi.org/10.1016/j.chroma.2021.462314

Mi, X., Wang, S.-C., Winters, M. A., & Carta, G. (2022). Protein adsorption on core-shell resins
for flow-through purifications: Effect of protein molecular size, shape, and salt
concentration. *Biotechnology Progress*, e3300. https://doi.org/10.1002/btpr.3300

Millipore. (2019). *Millistak+® Pod disposable depth filter system*.
https://www.emdmillipore.com/US/en/product/Millistak-HC-Pod-Depth-Filter-C0HC-me
dia-series-1.1m2-surface-area,MM_NF-MC0HC10FS1#overview

Millipore. (2023). *Charged Durapore® Cartridge 30 in. 0.22 μm Code 0 | CCGL03TP1*.
https://www.emdmillipore.com/US/en/product/Charged-Durapore-Cartridge-30in.-0.22m
-Code-0,MM_NF-CCGL03TP1

Mukhopadhyay, E., Brod, F., Angell-Manning, P., Green, N., Tarrant, R. D., Detmers, F. J.,

Bolam, E. J., Baleanu, I. N., Hobson, M., Whale, G., Morris, S. J., Ashfield, R., Gilbert,
S. C., Jin, J., Draper, S. J., Moyle, S. P., Berrie, E. L., & Hill, A. V. S. (2022). Production
of a high purity, C-tagged hepatitis B surface antigen fusion protein VLP vaccine for
malaria expressed in Pichia pastoris under cGMP conditions. *Biotechnology and
Bioengineering*, *119*(10), 2784–2793. https://doi.org/10.1002/bit.28181

Nadeem, A. Y., Shehzad, A., Islam, S. U., Al-Suhaimi, E. A., & Lee, Y. S. (2022). Mosquirix™
RTS, S/AS01 Vaccine Development, Immunogenicity, and Efficacy. *Vaccines*, *10*(5),
Article 5. https://doi.org/10.3390/vaccines10050713

National Institute of Health. (2020). *Drain Discharge Guide*.
https://nems.nih.gov/Documents/NIH_Drain_Discharge_Guide.pdf

National Research Council US Committee on Toxicology. (1984). *Emergency and Continuous
Exposure Limits for Selected Airborne Contaminants: Volume 2*.
https://www.ncbi.nlm.nih.gov/books/NBK208299/

Olotu, A., Fegan, G., Wambua, J., Nyangweso, G., Leach, A., Lievens, M., Kaslow, D. C.,
Njuguna, P., Marsh, K., & Bejon, P. (2016). Seven-Year Efficacy of RTS,S/AS01 Malaria
Vaccine among Young African Children. *New England Journal of Medicine*, *374*(26),
2519–2529. https://doi.org/10.1056/NEJMoa1515257

Oneko, M., Steinhardt, L. C., Yego, R., Wiegand, R. E., Swanson, P. A., Kc, N., Akach, D.,
Sang, T., Gutman, J. R., Nzuu, E. L., Dungani, A., Kim Lee Sim, B., Oloo, P. N., Otieno,
K., Bii, D. K., Billingsley, P. F., James, E. R., Kariuki, S., Samuels, A. M., … Seder, R.
A. (2021). Safety, immunogenicity and efficacy of PfSPZ Vaccine against malaria in
infants in western Kenya: A double-blind, randomized, placebo-controlled phase 2 trial.
Nature Medicine, *27*(9), Article 9. https://doi.org/10.1038/s41591-021-01470-y

Pall Corporation. (n.d.-a). *Allegro^{TM} STR Single-use Stirred Tank Bioreactors*. Retrieved March

    1, 2023, from https://shop.pall.com/us/en/biotech/cell-culture/bioreactors/zidhslqw8fu

Pall Corporation. (n.d.-b). *Allegro^{TM} XRS 25 Bioreactor System*. Retrieved March 1, 2023, from

    https://shop.pall.com/us/en/products/systems/zidhdf24174

Price, R. N., Commons, R. J., Battle, K. E., Thriemer, K., & Mendis, K. (2020). Plasmodium

    vivax in the Era of the Shrinking P. falciparum Map. *Trends in Parasitology*, *36*(6),

    560–570. https://doi.org/10.1016/j.pt.2020.03.009

Prpich, G. (2021a, April 22). *Scale-up of Bioreactor*.

Prpich, G. (2021b, August 20). *Growth Kinetics*.

Rachini, M. (2023, April 24). *A new malaria vaccine could be a "huge deal" in the fight to save*

    lives in Africa and abroad. CBC.

    https://www.cbc.ca/radio/thecurrent/malaria-vaccine-ghana-nigeria-who-1.6820289

Reimer, J. M., Karlsson, K. H., Lövgren-Bengtsson, K., Magnusson, S. E., Fuentes, A., &

    Stertman, L. (2012). Matrix-M^{TM} Adjuvant Induces Local Recruitment, Activation and

    Maturation of Central Immune Cells in Absence of Antigen. *PLoS ONE*, *7*(7), e41451.

    https://doi.org/10.1371/journal.pone.0041451

RTS,S Clinical Trials Partnership. (2015). Efficacy and safety of RTS,S/AS01 malaria vaccine

    with or without a booster dose in infants and children in Africa: Final results of a phase 3,

    individually randomised, controlled trial. *Lancet (London, England)*, *386*(9988), 31–45.

    https://doi.org/10.1016/S0140-6736(15)60721-8

Shen, C., Jacob, D., Shao, Z., Bernier, A., Yu, X., Patel, M., Zhu, T., & Kamen, A. (2015).

    Optimization and scale-up of cell culture and purification processes for production of an

    adenovirus-based tuberculosis vaccine. *BMC Proceedings*, *9*(9), 23.

https://doi.org/10.1186/1753-6561-9-S9-P23

SigmaAldrich. (n.d.). *Corning Erlenmeyer cell culture flasks 1 L Erlenmeyer Flask w/ Vent Cap,*

polycarbonate, sterile, 25/cs cell culture flasks. Retrieved March 1, 2023, from

http://www.sigmaaldrich.com/

Stratton, J., Chiruvolu, V., & Meagher, M. (1998). High Cell-Density Fermentation. In D. R.

Higgins & J. M. Cregg (Eds.), *Pichia Protocols* (pp. 107–120). Humana Press.

https://doi.org/10.1385/0-89603-421-6:107

Sub-Saharan Africa. (n.d.). The World Bank. https://data.worldbank.org/country/ZG

Talapko, J., Škrlec, I., Alebić, T., Jukić, M., & Včev, A. (2019). Malaria: The Past and the

Present. *Microorganisms*, *7*(6), 179. https://doi.org/10.3390/microorganisms7060179

The Engineering ToolBox. (2003). *Ethylene Glycol Heat-Transfer Fluid Properties*.

https://www.engineeringtoolbox.com/ethylene-glycol-d_146.html

The Engineering ToolBox. (2004). *Water—Saturation Pressure vs. Temperature*.

https://www.engineeringtoolbox.com/water-vapor-saturation-pressure-d_599.html

The Engineering ToolBox. (2005a). *Carbon Dioxide—Specific Heat of Gas vs. Temperature*.

https://www.engineeringtoolbox.com/carbon-dioxide-d_974.html

The Engineering ToolBox. (2005b). *Nitrogen Gas—Specific Heat vs. Temperature*.

https://www.engineeringtoolbox.com/nitrogen-d_977.html

The Engineering ToolBox. (2005c). *Oxygen Gas—Specific Heat vs. Temperature*.

https://www.engineeringtoolbox.com/oxygen-d_978.html

The Engineering ToolBox. (2005d). *Oxygen—Solubility in Fresh and Sea Water vs. Temperature*.

https://www.engineeringtoolbox.com/oxygen-solubility-water-d_841.html

The Engineering ToolBox. (2010). *Water—Heat of Vaporization vs. Temperature*.

https://www.engineeringtoolbox.com/water-properties-d_1573.html

Thermo Fisher Scientific. (2015). *CaptureSelect^TM Affinity Matrices – Column packing guidelines*. Thermo Fisher Scientific.

Thermo Fisher Scientific. (2017). *CaptureSelect^TM C-tagXL Affinity Matrix*. Thermo Fisher Scientific.

Thermo Fisher Scientific. (2020a). *Safety Data Sheet: Ultra Pure Tris Buffer*.

Thermo Fisher Scientific. (2020b). *Safety Data Sheet: 1% Triton X-100*.

Theron, C. W., Berrios, J., Steels, S., Telek, S., Lecler, R., Rodriguez, C., & Fickers, P. (2019). Expression of recombinant enhanced green fluorescent protein provides insight into foreign gene-expression differences between Mut+ and MutS strains of Pichia pastoris. *Yeast*, *36*(5), 285–296. https://doi.org/10.1002/yea.3388

Towler, G., & Sinnott, R. (2012). *Chemical Engineering Design: Principles, Practice and Economics of Plant and Process Design* (Second Edition). Elsevier Science & Technology.

United States Department of Agriculture. (2017). *Sodium Citrate*. https://www.ams.usda.gov/sites/default/files/media/SodiumCitrateCropsTR20171218.pdf

University of Oxford. (2023). *A Randomized, Open Label, Single Centre, Phase 2 Trial of the Malaria Vaccine, R21/Matrix-M, to Assess Safety and Immunogenicity of the Vaccine in Thai Adults* (Clinical Trial Registration No. NCT05252845). clinicaltrials.gov. https://clinicaltrials.gov/ct2/show/NCT05252845

von Stockar, U., & Birou, B. (1989). The heat generated by yeast cultures with a mixed metabolism in the transition between respiration and fermentation. *Biotechnology and Bioengineering, 34*(1), 86–101. https://doi.org/10.1002/bit.260340112

Wollborn, D., Munkler, L. P., Horstmann, R., Germer, A., Blank, L. M., & Büchs, J. (2022). Predicting high recombinant protein producer strains of Pichia pastoris MutS using the oxygen transfer rate as an indicator of metabolic burden. *Scientific Reports*, *12*(1), Article 1. https://doi.org/10.1038/s41598-022-15086-w

Zekar, L., & Sharman, T. (2022). Plasmodium Falciparum Malaria. In *StatPearls*. StatPearls Publishing. http://www.ncbi.nlm.nih.gov/books/NBK555962/

Zhang, R., Grimi, N., Marchal, L., & Vorobiev, E. (2019). Application of high-voltage electrical discharges and high-pressure homogenization for recovery of intracellular compounds from microalgae Parachlorella kessleri. *Bioprocess and Biosystems Engineering*, *42*(1), 29–36. https://doi.org/10.1007/s00449-018-2010-4

H. Appendix

Table H1

Literature Kinetic Growth Parameters on Different Substrates

	Glycerol	**Methanol**
K_m (g/L) [a]	0.10	0.34
μ_m (h^{-1})	0.22 [a]	0.14 [b]
$Y_{X/S}$ (g/g)	0.6 [a]	0.4 [c]
$Y_{P/S}$ (g/g)	0	0.00045 [d]
$Y_{X/O2}$ (g/mol O$_2$) [e]	47.82	10.54
$Y_{Q/O2}$ (kJ/mol O$_2$) [f]	440	440

[a] Canales et al., 2018
[b] Stratton et al., 1998
[c] Çelik et al., 2009
[d] Theron et al., 2019 - this $Y_{P/S}$ value is for a 55 kDa protein and serves as a conservative estimate
[e] Liang & Yuan, 2007
[f] von Stockar & Birou, 1989

Table H2

Chemical Balance-Derived Kinetic Growth Parameters on Different Substrates

	Glycerol	**Methanol**
$Y_{X/O2}$ (g/g)	1.89	0.54
$Y_{H2O/O2}$ (g/g)	1.21	1.00
RQ (g CO$_2$/g O$_2$)	1.05	0.67

Table H3

MGY Media Composition

Component	Quantity
WFI	700 mL
Potassium Phosphate Buffer	100 mL
10X YNB	100 mL
10X Glycerol	100 mL
500X Biotin	2 mL

Table H4

Basal Salts Media Composition

Component	Quantity
Phosphoric Acid (85%)	26.7 mL
Calcium Sulfate	0.93 g
Potassium Sulfate	18.2 g
Magnesium Sulfate - 7 H_2O	14.9 g
Potassium Hydroxide	4.13 g
Glycerol	40.0 g
WFI	1 L
PTM1 Trace Salts*	4.35 mL

*Note: Assume that PTM1 has no volume contribution and thus does not dilute the amount of

glycerol during fermentation.

Table H5

PTM1 Trace Salts Composition

Component	Quantity
Cupric Sulfate - 5 H_2O	6 g
Sodium Iodine	0.08 g
Manganese Sulfate - H_2O	3 g
Sodium Molybdate - 2 H_2O	0.2 g
Cobalt Chloride	0.5 g
Zinc Chloride	20 g
Ferrous Sulfate - 7 H_2O	65.0 g
Biotin	0.2 g
Sulfuric Acid	5 mL
WFI	1 L

Table H6

Glycerol Feed Composition

Component	Quantity
50% w/v Glycerol	1 L
PTM1	12 mL

Table H7

Methanol Feed Composition

Component	Quantity
100% Methanol	1 L
PTM1	12 mL

Table H8

Pichia Lysis Buffer Composition

Component	Concentrations (in WFI)	Quantity (1 L)
Triton	0.1 wt%	100 g
EDTA	1 mM	0.29 g
$MgCl_2$	1 mM	0.095 g
Tris	10 mM	1.21 g
WFI	-	1 L

Table H9

Annual Upstream Media and Substrate Usage

Material	Annual Quantity	Annual Cost
MGY Media	3.25 L	$30
Basal Salts Media	13000 L	$115,970
Glycerol Feed	945 L	$8,070
Methanol Feed	9450 L	$25,975
Total Cost of Media & Substrate		$150,045

Table H10

Annual Downstream Media, Buffer, and CIP Usage

Material	Annual Quantity	Annual Cost
PLB	14765 L	$121,950
WFI	42385 L	$778,955
CIP Solution (1 M NaOH in 30% isopropanol)	5990 L	$106,875
Sanitization Solution (0.5 M NaOH)	780 L	$4,955
Stripping Solution (Citric Acid)	820 L	$12,260
Affinity Equilibration Buffer	6535 L	$54,565
Elution Buffer 1	1635 L	$13,640
Elution Buffer 2	1635 L	$13,640
Total Cost of Media, Buffer, and CIP		$1,106,830

Note. WFI estimates account for the volume used directly in the purification process, cleaning, and equipment cooling.